Targeting plasmid-encoded proteins that contain immunoglobulin-like domains to combat antimicrobial resistance.

Alejandro Prieto[1*], Lluïsa Miró[2,3*], Yago Margolles[4], Manuel Bernabeu[1], David Salguero[1], Susana Merino[1], Joan Tomás[1], Juan Alberto Corbera[5], Anna Pérez-Bosque[2,3], Mário Hüttener[1], Luis Ángel Fernández[4] and Antonio Juárez[1,6**]

1. Department of Genetics, Microbiology and Statistics, University of Barcelona, Barcelona, Spain.

2. Department of Biochemistry and Physiology, Universitat de Barcelona, Barcelona, Spain.

3. Institut de Nutrició i Seguretat Alimentària, Universitat de Barcelona, Barcelona, Spain.

4. Department of Microbial Biotechnology, Centro Nacional de Biotecnología, Consejo Superior de Investigaciones Científicas (CNB-CSIC), Madrid, Spain.

5. Instituto Universitario de Investigaciones Biomédicas y Sanitarias (IUIBS), Facultad de Veterinaria, Universidad de Las Palmas de Gran Canaria (ULPGC), Campus Universitario de Arucas, Las Palmas, Spain.

6. Institute for Bioengineering of Catalonia, The Barcelona Institute of Science and Technology, Barcelona, Spain.

*Both authors contributed equally to this work.

**Corresponding author: Prof. Antonio Juárez, ajuarez@ub.edu

Running Title: Plasmid-encoded Big proteins targeted to combat antimicrobial resistance

Keywords: Antimicrobial resistance; IncHI plasmids; R27; Big proteins; RSP protein; vaccination; nanobodies; plasmid conjugation.

Abstract

Antimicrobial resistance (AMR) poses a significant threat to human health. Although vaccines have been developed to combat AMR, it has proven challenging to associate specific vaccine antigens with AMR. Bacterial plasmids play a crucial role in the transmission of AMR. Our recent research has identified a group of bacterial plasmids (specifically, IncHI plasmids) that encode large molecular mass proteins containing bacterial immunoglobulin-like domains. These proteins are found on the external surface of the bacterial cells, such as in the flagella or conjugative pili. In this study, we show that these proteins are antigenic and can protect mice from infection caused by an AMR *Salmonella* strain harboring one of these plasmids. Furthermore, we successfully generated nanobodies targeting these proteins, that were shown to interfere with the conjugative transfer of IncHI plasmids. Considering that these proteins are also encoded in other groups of plasmids, such as IncA/C and IncP2, targeting them could be a valuable strategy in combating AMR infections caused by bacteria harboring different groups of AMR plasmids. Since the selected antigens are directly linked to AMR itself, the protective effect extends beyond specific microorganisms to include all those carrying the corresponding resistance plasmids.

49 **Introduction**

50 Despite the availability of antibiotics, bacterial infectious diseases are the second leading cause
51 of death worldwide (Morens et al., 2004; Murray et al., 2022). The gradual increase in the
52 resistance rates of several important bacterial pathogens represents a serious threat to public
53 health (Meyer et al., 2010; Rossolini et al., 2007; Spellberg et al., 2008). In 2019, up to 4,95
54 million deaths could be associated to antimicrobial resistance (AMR) (Murray et al., 2022).

55 Plasmids can confer resistance to the major classes of antimicrobials (Carattoli, 2009). Their
56 transmission by horizontal gene transfer (HGT) is largely underlying the dissemination of AMR
57 genes, especially in Gram-negative bacteria (Carattoli, 2013; Thomas and Nielsen, 2005; Wang
58 et al., 2015), but also in Gram-positive bacteria (Vrancianu et al., 2020). Among the various
59 methods utilized for classifying plasmids, grouping them into incompatibility groups (Inc) is a
60 well-established and extensively employed approach (Novick and Richmond, 1965).

61 The incompatibility group HI includes plasmids that are widespread in the *Enterobacteriaceae*.
62 These plasmids frequently include genetic elements that encode multiple AMR determinants
63 (Phan and Wain, 2008). IncHI-encoded AMR can be present in enterobacteria such as *Salmonella*
64 (Phan and Wain, 2008), *Escherichia coli* (Forde et al., 2018), *Klebsiella pneumoniae* (Villa et al.,
65 2012), and *Citrobacter freundii* (Dolejska et al., 2013). Several *Salmonella* isolates harbor IncHI
66 plasmids, with those of the IncHI2 subgroup prevailing in antibiotic-resistant *Salmonella* isolates.
67 In *S. enterica* serotype Typhi, over 40% of isolates are found to carry an IncHI plasmid (Holt et
68 al., 2011). Recent reports have shown a novel role of IncHI plasmids in AMR spread. Colistin is a
69 last resort antibiotic for the treatment of severe infections (Lim et al., 2010). Plasmid-mediated
70 resistance, conferred by the mobilized colistin resistance gene (*mcr-1*), has emerged recently.
71 Approximately 20% of global isolates carrying the *mcr-1* gene are associated with an IncHI2
72 plasmid, and this percentage escalates to 41% when considering exclusively European isolates
73 (Matamoros et al., 2017). Of special concern is the presence of the *mcr-1* resistance determinant

74 in enterobacterial isolates carrying carbapenem resistance genes, such as *blaNDM* and *blaKPC*.
75 The combination of these AMR determinants can seriously compromise the treatment of
76 infections caused by virulent strains harboring these plasmids (Wang et al., 2017; Zheng et al.,
77 2016). An example of this is the recent report of an AMR clone of the highly virulent *E. coli* ST95
78 lineage (Forde et al., 2018). *E. coli* ST95 clones cause neonatal meningitis and sepsis. They are
79 usually sensitive to several antibiotics. This AMR clone harbors an IncHI2 plasmid that carries,
80 among other factors, genes encoding determinants of resistance to colistin and multiple other
81 antibiotics (including the extended-spectrum beta-lactamase $bla_{CTX\text{-}M\text{-}1}$ gene cluster). The spread
82 of such an AMR ST95 clone could pose a threat to human health worldwide (Forde et al., 2018).

83 The R27 plasmid is the best studied IncHI1 plasmid. It harbors the Tn10 transposon, which
84 confers resistance to tetracycline. The R27 replicative and conjugative machineries have been
85 studied in detail (Lawley et al., 2003, 2002) and its complete nucleotide sequence is known
86 (Sherburne et al., 2000). A newly reported feature of IncHI plasmids is that they code for large
87 molecular mass proteins that contain bacterial Ig-like (Big) domains (Hüttener et al., 2022, 2019).
88 Bacterial proteins containing Big domains play different roles in the cell. Some fimbrial subunits,
89 adhesins, membrane transporters and enzymes contain Big domains (as reviewed in (Bodelón
90 et al., 2013)). The IncHI1 plasmid R27 encodes the *rsp* and *rsp*2 genes which code respectively
91 for the 155.4 kDa RSP and 86.75 kDa RSP2 proteins. These proteins interact and target both the
92 flagella and the conjugative pili to favor conjugation (Hüttener et al., 2022). Big proteins are also
93 encoded at least by two other groups of plasmids (IncA/C and IncP2) (Hüttener et al., 2022). Due
94 to their extracellular location, these plasmid-encoded Big proteins could be considered as
95 valuable antigens to combat antimicrobial resistance.

96 Functional heavy-chain-only antibodies (HCAbs) were discovered nearly 30 years ago in the
97 serum of camelids (Hamers-Casterman et al., 1993). HCAbs lack both the light chains and the
98 first constant CH1 domain within the heavy chain. The variable domain of HCAbs, also termed

99 VHH for VH of HCAb, represents the smallest antigen-binding unit that occur in nature
100 (Muyldermans, 2013). The VHH domains can be expressed in recombinant form as highly stable
101 single-domain Ab fragments of ~14 kDa, also termed Nanobodies (Nbs), which exhibit high
102 affinity and specificity to its cognate antigens and unique recognition of cryptic epitopes not
103 recognized by conventional Abs (Muyldermans, 2013). Nbs can be easily produced in bacteria
104 and other microbial cultures, and used in multiple diagnostic and therapeutic applications,
105 including bacterial infections (Muyldermans, 2021).

106 In this study, our objective was to investigate the potential of the recently discovered Big
107 proteins encoded by IncHI plasmids as targets for combating antibiotic resistance. Our research
108 focused on two key aspects. First, we examined the efficacy of the RSP protein as a vaccine
109 antigen in providing protection against infections caused by resistant bacteria carrying an IncHI
110 plasmid. The results obtained confirmed the efficacy of the RSP protein as a vaccine antigen.
111 Furthermore, we also generated RSP-specific Nbs and showed that they can interfere with the
112 conjugative transfer of the R27 plasmid. Hence, the use of antigens that are directly linked to
113 AMR determinants can be effective in combating infections caused by AMR bacteria.

114 Results

115 Ampicillin protects mice from infection with the *S.* Typhimurium SL1344 (WT) strain, but not
116 from infection with the *S.* Typhimurium SL1344 (pHCM1) strain.

117 Considering the prevalence of IncHI plasmids in *Salmonella,* and the use of *S.* Typhimurium
118 infection in mice as a model for *Salmonella* infection, we employed a mouse infection model to
119 validate the RSP protein as a vaccine antigen against an antibiotic-resistant *Salmonella* strain.
120 For antibiotic treatment, we specifically selected ampicillin (Amp) due to its established efficacy
121 in reducing the symptoms of *Salmonella* infection in mice (Butler et al., 1981; Rossi et al., 2017).
122 For our study, we chose the IncHI plasmid pHCM1, which harbors an Amp resistance gene.

123 We first established that both *Salmonella* strains used (WT and pHCM1) were capable of
124 infecting mice, and that only the plasmid-bearing strain was antibiotic resistant. Infection with
125 the *Salmonella* strain SL1344 (WT) reduced the survival rate of the mice by about 40% (Fig. 1A),
126 while the addition of Amp increased the survival rate of these animals. On the other hand, Amp
127 treatment did not change the survival of mice infected with strain SL1344 (pHCM1).

128 In antibiotic-naive mice infected with either SL1344 (WT) or SL1344 (pHCM1) strains, gradual
129 weight loss and clinical signs of disease were observed (Figs. 1B and 1C). However, Amp
130 treatment only ameliorated these symptoms in mice infected with the SL1344 (WT) strain,
131 showing no effect on those infected with the SL1344 (pHCM1) strain. Additionally, infection with
132 both *Salmonella* strains led to an upregulation of proinflammatory cytokines in the spleen (Fig.
133 1D, 1E, 1F). Amp treatment in mice infected with the SL1344 (WT) strain prevented this increase
134 in cytokine expression.

135 **Immunization of mice with the RSP protein.**

136 We then purified the RSP protein and employed it as a vaccine antigen to evaluate its efficacy in
137 protecting mice against infection caused by the *S*. Typhimurium SL1344 strain carrying the
138 pHCM1 plasmid. To prevent the recurrence of infection by SL1344 clones that spontaneously
139 cured the pHCM1 plasmid in the absence of Amp, we maintained the antibiotic treatment in the
140 immunized animals.

141 The immunization process did not have a significant impact on the body weight progression of
142 the mice (Fig. 2A). Although the overall concentration of total serum IgG remained unchanged
143 following immunization (Fig. 2B), there was a substantial increase in the levels of specific IgG
144 antibodies against the RSP protein (Fig. 2C). In terms of intestinal IgA, immunization resulted in
145 an elevated concentration of total IgA in both the jejunum content and feces (Fig. 2D and 2H,
146 respectively), while not affecting its presence in the colon (Fig. 2F). Moreover, immunization led

147 to enhanced production of specific IgA antibodies against the RSP protein in all three tissue types
148 (intestinal contents Fig. 2E; colon contents Fig. 2G; and feces Fig. 2I).

149 **Effects of immunization of mice on the infection caused by the *S.* Typhimurium SL1344**
150 **(pHCM1) strain.**

151 Survival, body weight evolution and clinical signs

152 Infection with the SL1344 (pHCM1) strain resulted in a decrease in the survival rate of mice and
153 an approximate 20% reduction in their body weight after 6 days of infection. Additionally, it led
154 to an increase in the manifestation of clinical signs associated with infection (Fig. 3). However,
155 immunization significantly improved the survival rate of mice and reduced the incidence of
156 clinical signs in infected animals.

157 Intestinal effects of immunization with the RSP protein and challenge with the SL1344 (pHCM1)
158 strain

159 Immunization with the RSP protein increased the secretion of total IgA into the lumen of the
160 jejunum and colon (Figs. 4A and B), while reducing its concentration in feces (Fig. 4C).
161 Furthermore, immunization with the RSP protein led to an elevated presence of specific IgA
162 antibodies against the RSP protein in all three samples (Fig. 4D-F), with even higher levels
163 observed in infected animals in the case of fecal content. Regarding the expression of
164 proinflammatory cytokines, infection with the SL1344 (pHCM1) strain resulted in increased
165 expression of all three cytokines analyzed (Fig. 4G-I) both in immunized and non-immunized
166 animals. In the case of Tnf-α, immunization also increased its expression.

167 Systemic effects of immunization with the RSP protein and challenge with the SL1344 (pHCM1)
168 strain

169 The immunization protocol also resulted in an increase in the concentration of total IgG at the
170 systemic level (Fig. 5A), while infection with the SL1344 (pHCM1) strain reduced it. Additionally,
171 immunization also led to an elevated concentration of specific anti-RSP IgG in the serum (Fig.
172 5B), which remained unaffected after infection with the SL1344 (pHCM1) strain. Following
173 bacterial challenge, the spleen weight increased nearly threefold in non-immunized mice (Fig.
174 5C). In contrast, immunized mice exhibited a significantly lower increase in spleen weight.
175 Furthermore, animals infected with the SL1344 (pHCM1) strain displayed *Salmonella*
176 colonization in the spleen (Fig. 5D), which was significantly reduced in immunized animals.
177 Regarding the expression of proinflammatory cytokines in the spleen, *Salmonella* infection
178 upregulated the expression of all cytokines evaluated (Fig. 5E-G). Immunization partially
179 mitigated this effect on Il-1β and Tnf-α expression.

180 **Selection of nanobodies with neutralizing activity against the RSP protein**.

181 Given the protective effect against *Salmonella* infection observed in mice immunized with the
182 RSP protein, we wondered whether we could obtain specific antibodies against RSP that could
183 directly interfere with its biological activity in the conjugative transfer of IncHI plasmids. We
184 chose nanobodies as ideal candidates to block RSP activity given their small size, stability and
185 high affinity to antigens, and their therapeutic potential against infections. Interestingly,
186 nanobodies can also be expressed on the surface of *E. coli* fused to the initial 654 amino acids
187 of the enterohemorrhagic *E. coli* intimin protein, termed Neae (Bodelón et al., 2009), comprising
188 the N-terminal signal peptide, the periplasmic LysM domain, the β-barrel for outer membrane
189 insertion, and the extracellular Big domains D00 and D0 (Fairman et al., 2012). Expression of
190 Neae-Nb fusions represent an efficient bacterial display system for their selection of Nbs binding
191 a target antigen from VHH gene libraries employing *E. coli* cell sorting methods with the labelled
192 antigen (Salema et al., 2013; Salema and Fernández, 2017). In addition, Neae-Nb fusions

193 expressed in *E. coli* promote synthetic cell-to-cell adhesions mediated by the specific recognition
194 of a surface antigen in the target cell (Glass and Riedel-Kruse, 2018; Piñero-Lambea et al., 2015).
195 In order to obtain Nbs that specifically bind the extracellular domain of the RSP protein, we
196 immunized two dromedaries with the last 280 residues of the C-terminal domain of the RSP
197 protein. After immunization, peripheral blood lymphocytes from these animals were isolated
198 and the VHH gene segments were amplified and cloned in the display vector pNeae2 (Robledo
199 et al., 2022; Salema et al., 2013), which encodes the Neae intimin fragment under the control of
200 the IPTG-inducible lacI-Plac promoter region. A library of approximately $1x10^8$ clones was
201 obtained by electroporation of *E. coli* DH10BT1R strain with the products of the ligated pNeae2-
202 VHH. Bacteria in library were grown in liquid culture and induced with IPTG. Induced bacteria
203 binding the C-domain of RSP were selected by incubation with the purified protein labeled with
204 biotin, following iterative steps of magnetic cell sorting (MACS) and fluorescence-assisted cell
205 sorting (FACS) (Materials and Methods). After the final sorting step (Fig. 6A), the selected pool
206 of bacteria was grown on LB-agar plates. 96 colonies were randomly picked from these plates,
207 grown in liquid, and induced with IPTG to evaluate the Nb display levels on the bacterial surface
208 and their binding capability to the biotinylated C-domain of the RSP protein by flow cytometry
209 (Fig. 6B). The VHH sequences from clones with specific binding to purified RSP were determined,
210 which allowed us to identify 7 different Nbs (Supplementary Fig. 1).

211 **Selection of Nb clones displayed on *E. coli* that agglutinate with the *S.* Typhimurium SL1344**
212 **(R27) strain.**

213 For selection of Nbs binding native RSP expressed on *Salmonella* cells, we took advantage of the
214 specific adhesion observed between *E. coli* cells with displayed Nbs and bacteria having the
215 target antigen accessible on their surface, which leads to the agglutination of mixed bacterial
216 cultures (Glass and Riedel-Kruse, 2018; Robledo et al., 2022).
217 We initially evaluated the agglutination capability of the 7 different clones obtained in the
218 enrichment protocol of the immune library, from strain *E. coli* DH10BT1R, each carrying a

219 pNeae2-VHH derivative expressing RSP-specific Nbs, against the *S*. Typhimurium SL1344 (R27)
220 strain. To achieve this, we cultured the *Salmonella* strain in LB medium to an $OD_{600\ nm}$ of 2.
221 Following centrifugation, cells were resuspended in PBS and mixed with an equal volume of a
222 culture of the different *E. coli* DH10BT1R clones displaying the different set of RSP-specific Nbs.
223 Only one of the clones tested (Nb 3) showed ability of agglutinating the *S*. Typhimurium SL1344
224 (R27) strain (Fig. 7A). Next, we inspected this phenomenon using electron microscopy (Fig. 7B)
225 The presence of the R27 plasmid dictated the formation of clumps between the SL1344 strain
226 and *E. coli* DH10BT1R (pNeae2 VHH-RSP #3). In contrast, no clumps or aggregates were observed
227 when the plasmid-free SL1344 or the SL1344 (R27 Δ*rsp*) strains were used.
228 To further characterize this clone, the corresponding VHH gene was cloned in the mammalian
229 expression vector pIgΔCH1 (Casasnovas et al., 2022), which allows the fusion of the selected Nb
230 domain to the Fc region of human IgG1. The corresponding Nb3-Fc protein fusion was purified
231 from culture supernatants of transfected Expi293F cells (Fig. 8A), and its binding capacity to the
232 RSP protein was analyzed by ELISA. The results indicated that this Nb3-Fc presented a high
233 affinity for binding to the RSP protein, showing an apparent equilibrium dissociation constant
234 (K_D) in the picomolar range (~44 pM) (Fig. 8B).

235 **Interference of *E. coli* displaying Nb-RSP #3 strain on the conjugation of the R27 plasmid from**
236 **the *Salmonella* Typhimurium SL1344 strain.**

237 Our objective was to investigate whether the *E. coli* surface expression of the Nb-RSP #3 would
238 be able interfere with the conjugation process of the R27 plasmid from the SL1344 *Salmonella*
239 strain (donor) to the SL1344 *ibpA::lacZ-Km*^{r} derivative (recipient). To prevent that the Nbs
240 produced by the *E. coli* DH10BT1R (pNeae2 VHH-RSP #3) were titrated out by an excess of
241 SL1344 (R27) donor cells, we planned a conjugation experiment with a low number of donor
242 cells (10^3 cfu) mixed with an abundance of recipient cells (SL1344 *ibpA::lacZ-Km*^{r}) (10^6 cfu), along
243 with an excess of cells corresponding to the *E. coli* strain displaying Nb-RSP #3 (10^7 cfu).

244 Considering the known conjugation frequency of the R27 plasmid in *Salmonella* at 25°C, which
245 is approximately 10^{-3}, and the low number of donor cells used in our experiment, we chose
246 specific time intervals of 24, 36 and 48 hours following the mating process to detect
247 transconjugants within the mating mixture. To accomplish this, the mating mixture was mixed
248 with PB medium and incubated at 25°C. To confirm that any effect on the conjugation frequency
249 was solely due to the production of RSP-specific Nbs and not to other non-specific effects of Nb
250 expression, we utilized as controls both a plasmid-free *E. coli* DH10BT1R strain and the same
251 strain displaying an unrelated Nb binding human fibrinogen (Salema et al., 2016). The results
252 obtained (Fig. 9) indicated that the surface display of Nb-RSP #3 by the interfering *E. coli* strain
253 led to a significant and specific reduction in the conjugation frequency of the R27 plasmid in the
254 *S.* Typhimurium SL1344 strain. Interfering *E. coli* strains with no Nb or a control Nb elicited a
255 nonspecific ~10-fold reduction in the number of transconjugants of R27 plasmid in all time
256 points, compared to conjugation levels between *Salmonella* SL1344 strains. In contrast,
257 interfering *E. coli* displaying Nb-RSP #3 reduced the number of transconjugants of R27 up to
258 ~1000-fold at 24h and ~100-fold after 36 and 48h of mating (Fig. 9). These results suggest a
259 strong inhibitory effect in the conjugation of R27 due to the interaction between bacterial
260 display Nb-RSP #3 and RSP protein expressed by donor cells. To rule out that the observed
261 reduction in the conjugation frequency in mixtures containing the *E. coli* strain DH10BT1R
262 (pNeae2 VHH-RSP #3) and the SL1344 (R27) strains could be due to the specific transfer of the
263 R27 plasmid to the interferent *E. coli* DH10BT1R (pNeae2 VHH-RSP #3) strain, we also detected
264 transconjugants of the *E. coli* DH10BT1R (pNeae2 VHH-RSP #3) and *E. coli* DH10BT1R (pNVFib1)
265 interferent strains by plating them on LB medium containing Tc (R27 plasmid marker) and Cm
266 (pNeae2 plasmid marker). In both experiments the conjugation frequency was the same ($1.5x10^{-}$
267 ^{2} transconjugants/donor cells).

268 **Discussion**

269 Vaccination stands as a priority strategy in addressing the challenges posed by AMR (Frost et al.,
270 2022; Micoli et al., 2021). Vaccines of special interest should target the agents responsible for
271 significant health care-associated infections, which include multiple resistant Gram-negative
272 bacteria (Lipsitch and Siber, 2016). Protecting against specific pathogens (i.e., *S. pneumoniae, K.*
273 *pneumoniae*) reduced the incidence of infections caused by them, leading to a decrease in
274 antibiotic usage and hence reducing the proliferation of AMR strains (Buchy et al., 2020).

275 One of the challenges in vaccine development is the identification of broadly protective antigens
276 (Troisi et al., 2020). In the context of AMR, current strategies focus on targeting either the most
277 common antigens among AMR clones of a specific pathogen (Micoli et al., 2021) or specific
278 virulence determinants (Moriel et al., 2010; Nesta et al., 2012). However, an alternative
279 approach is to develop a vaccine that directly targets a resistance determinant, which would be
280 effective not only against a specific microorganism but also against any microorganism
281 expressing the corresponding resistance determinant. Examples of successful targeting include
282 penicillin-binding proteins or beta-lactamases, which have demonstrated protection against
283 infections caused by *Staphylococcus aureus* (Senna et al., 2003), *Neisseria meningitidis*
284 (Zarantonelli et al., 2006), or *Pseudomonas aeruginosa* (Ciofu et al., 2002).

285 The novelty of the approach presented in this work is that, instead of targeting an antigen
286 involved in an antibiotic resistance mechanism, we focus on an antigen associated with the
287 transmission of resistance determinants.

288 Big proteins have been previously shown to be good vaccine candidates (Khanum et al., 2022;
289 Koizumi and Watanabe, 2004). The antigenicity of the RSP protein has been demonstrated by
290 the presence of higher levels of specific immunoglobulins. Immunized mice exhibited higher
291 levels of IgG in serum and IgA in the colon, jejunum, and feces compared to control mice. In
292 terms of the protective effect of immunization with the RSP protein in mice, the results can be
293 interpreted as follows. The secretion of proinflammatory cytokines in the colon was comparable

294 between immunized and non-immunized animals, as well as the reduction in body weight.
295 However, clinical symptoms, *Salmonella* counts in the spleen, and the weight and secretion of
296 proinflammatory cytokines in this organ were significantly reduced in immunized animals. While
297 immunization with the RSP protein did not provide complete protection against intestinal
298 infection with the SL1344 strain, it did result in attenuated disease symptoms and restricted
299 systemic infection. These findings support further research to validate the RSP protein as a
300 valuable antigen for protection against bacterial infections caused by enteric bacteria harboring
301 IncHI plasmids.

302 IncHI plasmids are commonly found in AMR bacteria isolated from clinical samples (Parvez and
303 Khan, 2018; Zhang et al., 2021). They are also frequently identified in *Salmonella* isolates (Phan
304 and Wain, 2008). The emergence of AMR *S. typhi* isolates has been reported in developing
305 countries (Tanmoy et al., 2018). Developing an effective vaccine against this pathogen would be
306 particularly beneficial for children in endemic countries, including regions such as South Asia,
307 Southeast Asia, and sub-Saharan Africa, as well as for travelers (World Health Organization,
308 2019). The RSP protein shows promise as a valuable antigen to be included in such a vaccine,
309 offering potential protection against AMR *Salmonella* infections associated with IncHI plasmids.

310 An alternative approach to provide protection against infections caused by virulent AMR strains
311 carrying IncHI plasmids is to specifically target the RSP protein with antibodies. Monoclonal
312 antibodies against various bacterial pathogens have demonstrated effectiveness, with some
313 currently in advanced stages of clinical trials (Cook and Wright, 2022). Nanobodies, a novel class
314 of antibodies, offer a wide range of clinical applications (Graf et al., 2019; Jovčevska and
315 Muyldermans, 2020a). The use of nanobodies specifically targeting the RSP protein represents
316 a promising approach to combat infections caused by pathogenic bacteria harboring IncHI
317 plasmids. Inhibiting the transfer of antimicrobial resistance plasmids has been identified as a
318 crucial strategy to combat AMR (Buckner et al., 2018; Graf et al., 2019). Our study demonstrates

319 that *E. coli* strains producing RSP-specific nanobodies can bind to *Salmonella* cells carrying the
320 R27 plasmid, resulting in a reduction in the conjugation frequency.
321 These results reinforce the notion that expressing RSP-specific nanobodies in a probiotic
322 bacterium, such as *E. coli* Nissle 1917, could potentially limit the transfer of IncHI plasmids in
323 natural settings, such as livestock farms. Furthermore, RSP-specific antibodies could be utilized
324 to combat infections caused by pathogenic isolates carrying IncHI plasmids. Nanobodies, known
325 for their heat- and acid-stability and solubility, show potential for oral administration to control
326 gastrointestinal infections (Yuki et al., 2023). Thus, either purified RSP-specific nanobodies or
327 probiotic microbial cells expressing these nanobodies could be orally administered to combat
328 infections caused by AMR virulent strains harboring IncHI plasmids.

329 The expression of plasmid-encoded Big proteins is not exclusive to IncHI plasmids; other
330 plasmids such as IncA/C and IncP2 also encode these proteins (Hüttener et al., 2022). IncA/C
331 plasmids were initially identified in the 1970s among multidrug-resistant *Aeromonas hydrophila*
332 and *Vibrio* strains that infected cultured fish (Aoki et al., 1971). Since the 1990s, IncA/C plasmids
333 have gained significant attention due to their ability to mobilize antimicrobial resistance
334 determinants in enterobacteria and other Gram-negative microorganisms (Call et al., 2010;
335 Fernández-Alarcón et al., 2011; Fricke et al., 2009; Welch et al., 2007). These plasmids have an
336 exceptionally wide host range, encompassing Beta-, Gamma-, and Deltaproteobacteria (Suzuki
337 et al., 2010), and they play a crucial role in the global dissemination of antimicrobial resistance
338 (Eda et al., 2020; Rozwandowicz et al., 2018). In a recent study, IncA/C plasmids accounted for
339 50% of all plasmids isolated from clinical *K. pneumoniae* strains harboring the *blaNDM* gene
340 (Qamar et al., 2021). Notably, the monophasic variant of *S*. Typhimurium, *S. enterica* serovar
341 4,[5],12:i:-, which has emerged as a global cause of multidrug-resistant salmonellosis,
342 predominantly harbors IncHI1 and IncA/C resistance plasmids (Ingle et al., 2021).

343 Therefore, targeting these plasmid-encoded Big proteins through immunotherapies can be a
344 valuable strategy to combat infections caused by pathogenic microorganisms carrying various
345 types of resistance plasmids.

346 ## Methods

347 **Bacterial strains and growth conditions.**

348 The bacterial strains (see Supplementary Table S1) were routinely grown in Luria-Bertani (LB)
349 medium (10 g/L NaCl, 10 g/L tryptone and 5 g/L yeast extract) with vigorous shaking at 200 rpm
350 (Innova 3100; New Brunswick Scientific). The antibiotics used were chloramphenicol (Cm) (25
351 µg/mL), tetracycline (Tc) (15 µg/mL), carbenicillin (Cb) (100 µg/mL), and kanamycin (Km) (50
352 µg/mL) (Sigma-Aldrich). *E. coli* strains carrying the plasmid with a VHH gene were grown at 30ºC
353 on LB-agar plates (1.5% w/v) or in LB liquid medium with the addition of chloramphenicol (Cm,
354 30 µg/mL) for plasmid selection. To overexpress the nanobodies in the bacterial surface of *E.*
355 *coli* DH10BT1R, firstly bacteria were grown overnight (O/N) under statics conditions in LB
356 medium containing 2% (w/v) of glucose. Then, bacteria were harvested by centrifugation (4000
357 g for 5 minutes) and grown in the same media supplemented with 0.05 mM isopropylthio-β-D-
358 galactoside (IPTG) in constant agitation (160 rpm) for 16 hours.

359 **Plasmids.**

360 The different plasmids used in this work are listed in Supplementary Table S1.

361 **Oligonucleotides.**

362 The oligonucleotides used in this work are listed in Supplementary Table S2.

363 **Genetic manipulations.**

364 All enzymes used to perform standard molecular and genetic procedures were used according
365 to the manufacturer's recommendations. To introduce plasmids into *E. coli, Salmonella* and
366 *Klebsiella*, bacterial cells were grown until an $O.D_{600\ nm}$ of 0.8. Cells were then washed several

367 times with 10% glycerol, and the respective plasmids or DNA were electroporated by using an
368 Eppendorf gene pulser (Electroporator 2510).
369 Deletion of the *flhDC* locus was performed in the strain SL1344 by using the λ Red recombination
370 method, as previously described (Datsenko and Wanner, 2000).
371 **Conjugative transfer of the R27 plasmid**.

372 The R27 plasmid was conjugated as described previously (Hüttener et al., 2019). The mating
373 frequency was calculated as the number of transconjugants per donor cell.

374 **Purification of the native RSP protein for the immunization assay.**

375 The RSP protein was purified from cell-free supernatant fractions obtained from the *Salmonella*
376 cells lacking the flagella (SL1344 R27 *flhDC::Km*). Cells were grown at 25ºC in LB medium for 16
377 hours in constant shaking at 200 rpm, then centrifugated at 7000 rpm for 30 minutes at room
378 temperature. Cell pellets were discarded, and the supernatant was filtered through a 0.22 μm
379 filter (Millipore). Supernatants were then ultra-centrifugated at 40000 rpm for 1 hour at 4ºC and
380 carefully aspired to not disturb the protein pellet and discarded. The remaining pellet was
381 solubilized using commercial Phosphate-buffered saline (PBS – Gibco). Proteins were quantified
382 using the Bradford standard method (Pierce).

383 **Purification of the C-terminal domain of the RSP protein.**

384 For the RSP protein production the carboxyl-terminal region of the RSP protein was amplified
385 (280 AA in total). Amplification of that region was achieved by performing PCR using the R27
386 plasmid as a DNA template and the primers RSP5 BamHI Fw and RSP PstI Rv, together with the
387 Phusion Hot Start II High-fidelity DNA Polymerase (Thermo Fisher Scientific) following the
388 manufacturer's recommendations. The DNA was then purified using the GeneJet PCR
389 Purification Kit (Thermo Fisher Scientific), digested with BamHI and PstI restriction
390 endonucleases according to the manufacturer´s instructions (New England Biolabs), and ligated

391 into the pMAL-p2E vector digested with the same restriction endonucleases using the T4 DNA
392 Ligase (New England Biolabs) according to the manufacturer´s instructions. The resulting
393 plasmid, termed pMAL-RSP#5/7, was Sanger sequenced and transformed into BL21 cells. Cells
394 transformed with pMAL-RSP#5/7 plasmid were grown in LB medium supplemented with
395 carbenicillin at a final concentration of 100 µg/mL at 37°C for 16 hours at constant agitation at
396 200 rpm. Then, cells were diluted 1:100 in LB with 100 µg/mL of carbenicillin and glucose at
397 0.45% of the final concentration. Cells were incubated at 37ºC with 200 rpm until reached the
398 $O.D_{600\ nm}$ of 0.5, then IPTG was added at a final concentration of 0.15 mM. Cells were incubated
399 at 37ºC for 2 hours under constant agitation of 200 rpm for the induction of the recombinant
400 protein. Cells were then centrifuged at 7500 rpm for 30 minutes at 4°C. The cells pellet was
401 subsequently resuspended in column buffer (20 mM HEPES (Na) pH 7.5, 200 mM NaCl, 1 mM
402 EDTA, 1 mM β-mercaptoethanol) plus protease inhibitor (Complete Ultra Tablets, Mini, EDTA-
403 free, EASYpack, Roche). Cells were then disrupted by French press cell lysis and centrifugated at
404 12000 rpm for 1 hour at 4°C. Supernatants were filtered through a 0.22 µM filter (Millipore) and
405 mixed with 250 µl of Amylose resin (New England Biolabs) for 2 hours at 4ºC in an orbital shaker.
406 The resin was then loaded in chromatography columns and washed twice with the column
407 buffer. The recombinant RSP C-terminal protein was then eluted using the elution buffer (20
408 mM HEPES (Na) pH 7.5, 200 mM NaCl, 1 mM EDTA, 1 mM β-mercaptoethanol and 10 mM
409 maltose). Eluted fractions were collected and then concentrated using Amicon Ultra-15 Ultracel
410 10K (Millipore) according to the manufacturer´s instructions.

411 **Immunization of dromedaries with the C-terminal fragment of the RSP protein and selection**
412 **of clones producing anti-RSP specific nanobodies.**

413 Two different dromedary camels (*Camelus dromedarious*) were immunized with purified RSP
414 protein (~1.2 mg) mixed with veterinary vaccine adjuvant (GERBU). After 6 rounds of
415 inoculations by subcutaneous injections, serial dilutions of pre-immune and immune sera were

416 used in ELISA to confirm the immune response of dromedary after the RSP protein inoculation.
417 B lymphocytes from peripheral blood were isolated, RNA was extracted and VHH genes were
418 amplified by RT-PCR using the VHH Sfi and VHH Not oligonucleotides following the protocol
419 described previously (Salema et al., 2013).

420 The amplified VHH fragments were digested with SfiI and NotI restriction enzymes and ligated
421 into the pNeae2 backbone vector digested with the same restriction enzymes, and finally
422 transformed in *E. coli* DH10BT1R by electroporation. Following this protocol, a library of $8.75x10^7$
423 clones was obtained.

424 This library was used for the enrichment of clones that recognized the RSP protein. To this end,
425 purified RSP protein was mixed with Biotin-NHS (Biotinamidocaproate N-hydroxysuccinimide
426 ester, Sigma Aldrich) and three rounds of MACS (with RSP concentrations of 100 nM (the first
427 one) and 50 nM (the other two)) were performed. Thereafter, a FACS selection with a protein
428 concentration of 50 nM were performed). The positive clones for the RSP binding were selected
429 for further analysis.

430 **Cloning and purification of the RSP specific nanobody (VHH-RSP #3).**

431 The gene coding for the RSP-specific selected Nb was PCR amplified with oligonucleotides VHH
432 pIg AgeI and VHH pIg BamHI using the pNeae2 VHH-RSP #3 purified plasmid as a template. This
433 PCR product was subsequently cloned in AgeI-BamHI sites of the mammalian expression vector
434 pIgΔCH1 (Casasnovas et al., 2022) derived from pIgγ1HC (Tiller et al., 2008). This vector allows
435 the expression of the cloned gene located in frame with a IgH signal peptide fused to the human
436 IgG1 hinge and Fc portion. For the nanobody overexpression and purification, the Expi293™
437 Expression System Kit (Thermo Fisher Scientific) was used. The mammalian cells transfected with
438 the purified expression vector (pIgΔCH1 VHH-RSP) were grown 5 days post-transfection. Cells
439 were then centrifuged, the supernatant was collected and filtered, and the proteins were

440 purified with an Ig Select or protein A affinity columns (Cytiva), following manufacturer's
441 instructions.

442 **Enzyme-linked immunosorbent assays to evaluate the specific VHH-RSP #3 binding to the RSP**
443 **protein.**

444 ELISA experiments were performed in 96-well plates (Maxisorp, Nunc), which were previously
445 coated overnight at 4°C with 50 µl/well of the purified RSP protein antigen or BSA at 3 µg/ml in
446 PBS. Antigen-coated plates were washed with PBS and blocked with 200 µl/well of 3% (w/v)
447 skimmed milk in PBS at room temperature for 2 h. Afterwards, different dilutions of the VHH-
448 RSP (prepared in 3% (w/v) skimmed milk in PBS) were added to the wells for 1 h. After the
449 incubation, the wells were washed three times with PBS, and rabbit anti-human Fc IgG-HRP
450 (Jackson ImmunoResearch) was added to the plates (diluted 1:5000 in 3% (w/v) skimmed milk
451 in PBS) to detect the bound Nbs. After 1 h of incubation at room temperature, plates were
452 washed with PBS and developed with H_2O_2 and o-phenylenediamine (OPD; Merck-Sigma). The
453 Optical Density (OD) at 490 nm ($OD_{490\ nm}$) of plate wells was determined (iMark, Bio-Rad), and
454 the values were corrected with the background levels of OD_{490nm} of the wells without antigen
455 added.

456 ***In vivo* immunization and infection of mice.**

457 Male and female C57BL/6 mice were purchased from Envigo (Bresso, Italy) and maintained
458 under stable temperature and humidity conditions with a 12-hour light 12-hour dark cycle and
459 free access to food and water.

460 <u>Set up of the infection protocol with the SL1344 (pHCM1) strain.</u>

461 To induce infection, the *S.* Typhimurium strain SL1344 (pHCM1) was chosen. An assay was
462 designed to assess whether infection with this strain is similar to infection with the plasmid-free
463 strain. Four groups of mice were infected with strains SL1344 and SL1344 (pHCM1), and two of

464 them were treated with 150 mg/kg/day ampicillin (Amp) (Sigma-Aldrich) in drinking water and
465 two of them were untreated. In addition, a group of uninfected control mice was included as a
466 reference group. Thus, the groups were: i) Control: uninfected mice; ii) Sal: SL1344-infected mice
467 not treated with Amp; iii) Sal-pHCM1: SL1344-pHCM1-infected mice not treated with Amp; iv)
468 Sal WT + Amp: SL1344-infected mice treated with Amp; v) Sal pHCM1 + Amp: SL1344-pHCM1-
469 infected mice treated with Amp. Three hours before the challenge with the bacterial suspension,
470 mice received an intraperitoneal injection of cimetidine (50 mg/kg; Sigma-Aldrich) to reduce acid
471 secretion and improve bacterial survival(Ren et al., 2014). To induce infection, 100 µl of the
472 bacterial suspension (10^9 cfu of *Salmonella*) was administered by oral gavage. During the
473 infection period the body weight of animals was monitored daily. Four to six days after infection
474 (depending on survival), the animals were evaluated for clinical signs of disease and fecal
475 samples were obtained. They were subsequently euthanized and samples of spleen, colon
476 mucosa, intestinal lavage and serum were obtained. Samples were obtained and processed as
477 described previously (Miró et al., 2023).

478 The parameters analyzed to score the clinical signs were: Coat care (normal, 0; slightly altered,
479 1; considerably altered, 2; very altered, 3); posture (normal, 0; slightly curved, 1; considerably
480 curved, 2; very curved, 3); movement (normal, 0; slightly slow, 1; considerably slow, 2; very slow,
481 3); defecation (normal, 0; soft stools, 1; watery stools, 2; liquid stools, 3); body weight loss (no
482 weight loss, 0; weight loss less than 5%, 1; weight loss between 5 and 10%, 2; weight loss greater
483 than 10%, 3).

484 <u>Immunization with the RSP protein and infection with the *S.* Typhimurium SL1344 (pHCM1)</u>
485 <u>strain.</u>

486 Regarding the adjustment of the immunization with the RSP protein as antigen, we proceeded
487 as previously described (Miró et al., 2023). Briefly, mice were intranasally administered with 3
488 µg of the RSP protein and 5 µg of cholera toxin (CT; Sigma-Aldrich) as immunological adjuvant.

489 Immunization was performed 3 times every 2 weeks (at 3, 5 and 7 weeks of age). Non-
490 immunized mice received CT alone. Mice were distributed randomly into two groups: Non-Imm
491 (Non-immunized, CT alone); Imm (Immunized mice). During the immunization period the body
492 weight of animals was monitored weekly. Two weeks after last immunization, animals were
493 euthanized and samples of feces, intestinal lavage and serum were obtained. Total and RSP-
494 specific immunoglobulins were determined as explained in the section Immunoglobulin
495 determination.

496 In order to evaluate the protective efficacy of immunization, the previously established infection
497 protocol with the *S.* Typhimurium SL1344 (pHCM1) strain was used. The experiments were
498 performed using a Latin design with two factors: immunization of mice using the RSP protein as
499 immunogen; and subsequently infected with the *S.* Typhimurium SL1344 (pHCM1) strain. The
500 animals were randomly distributed into four groups: i) non-immunized and non-infected mice
501 (Non-Imm); ii) non-immunized and *Salmonella*-infected animals (Sal); iii) immunized and non-
502 infected animals with *Salmonella* (Imm); iv) immunized and infected animals (Imm-Sal). The
503 infection was provoked two weeks after last immunization dose.

504 **Bacterial counts in spleen.**

505 Spleen samples were homogenized with sterile PBS (20 mg/mL) using a PRO200 homogenizer
506 (Pro-Scientific, USA) at 18000 g, and homogenates were used to count the presence of
507 *Salmonella* cells plated in MacConkey media agar plates.

508 **Immunoglobulin concentration.**

509 Total secreted IgA and anti-RSP-specific IgA were determined in intestinal and colon content and
510 in feces by sandwich enzyme-linked immunosorbent assay (ELISA) as previously described (Ren
511 et al., 2014). Briefly, plates were coated with anti-mouse IgA monoclonal antibody (1 µg/mL;
512 Sigma-Aldrich) in PBS to quantify total IgA concentration or RSP (20 µg/mL) in PBS to measure

513 RSP-specific IgA concentration. Mouse IgA (Bethyl) was used as a standard for the determination
514 of total IgA. Goat anti-mouse IgA (Bethyl) conjugated with horseradish peroxidase (HRP) was
515 used as the detection antibody.

516 The concentrations of total IgG and specific IgG against the RSP protein in serum were also
517 determined. Plates were coated with goat anti-mouse IgG (1 µg/mL; Sigma-Aldrich) to quantify
518 the concentration of total IgG or RSP (10 µg/mL) in PBS to measure the concentration of specific
519 IgG against RSP. Mouse IgG (Sigma-Aldrich) was used as a standard for the determination of
520 total IgG. Goat anti-mouse IgG conjugated with HRP (Sigma-Aldrich) was used as detection
521 antibody.

522 In all cases, o-phenylenediamine (OPD, 0.4 mg/mL; Sigma-Aldrich) was used as HRP substrate,
523 and the color intensity was measured at 492 nm in a microplate reader (Sunrise).

524 **Cytokine expression in spleen and colon.**

525 RNA extraction and reverse transcription were carried out as previously described (Rosell-
526 Cardona et al., 2022). RNA quality and quantity were assessed by spectrophotometry (NanoDrop
527 ND-1000; Thermo Fisher Scientific) and its integrity was determined with an Agilent 2100
528 Bioanalyzer (Agilent Technologies Inc.). In all cases, the RNA integrity was ≥ 9 and the A260/280
529 ratio was between 1.96 and 2.02. Total RNA was reverse-transcribed using an iScript™ cDNA
530 Synthesis Kit (Bio-Rad). For real-time PCR determinations, we used SsoAdvanced™ Universal
531 SYBR® Green Supermix (Bio-Rad). The primers used are described previously (Garcia-Just et al.,
532 2020). Real-time PCR was performed on a MiniOpticon Real-Time PCR System (Bio-Rad). Each
533 PCR run included duplicates of reverse transcript cDNA for each sample and negative controls
534 (reverse transcription-free samples, RNA-free sample). Quantification of the target gene
535 transcripts was conducted using hypoxanthine phosphoribosyl transferase 1 (*hprt1*) gene
536 expression as reference and was performed with the $2^{-\Delta\Delta CT}$ method (Schmittgen and Livak,
537 2008). Product fidelity was confirmed by melting curve analysis.

538 **Immunogold electron microscopy.**

539 Immunogold microscopy experiments were performed as previously described (Hüttener et al.,
540 2019).

541 **Statistical analysis.**

542 The results of mice experiments are presented as mean ± SEM, except for survival curves and
543 disease indices. Survival curves have been compared by Log-rank (Mantel-Cox) test and
544 expressed as a percentage of survival. Disease indices are expressed as median values and
545 quartiles and have been compared by the Kruskal-Wallis test. Continuous data were analyzed
546 with Levene's test to assess the homogeneity of variance and with the Shapiro-Wilk test to
547 assess distribution. Homogeneous and normally distributed data were analyzed with Student's
548 t-test (immunization-tuning experiments) or one-way analysis of variance (ANOVA) (infection-
549 tuning) followed by Fisher's least significant difference (LSD) post hoc test and two-way ANOVA
550 (immunization and infection experiments). Student's t-test was also used to determine
551 statistical significance of R27 conjugation frequency in mating experiments. Data were analyzed
552 using GraphPad Prism® software v.9.3.1 (GraphPad Software, Inc.). Differences were considered
553 significant at $P<0.05$.

554 **References**

555 Aoki T, Egusa S, Kimura T, Watanabe T. 1971. Detection of R factors in naturally occurring
556 *Aeromonas salmonicida* strains. *Appl Microbiol* **22**:716–717. doi:10.1128/aem.22.4.716-
557 717.1971

558 Bodelón G, Marín E, Fernández LA. 2009. Role of Periplasmic Chaperones and BamA
559 (YaeT/Omp85) in Folding and Secretion of Intimin from Enteropathogenic *Escherichia coli*
560 Strains. *J Bacteriol* **191**:5169–5179. doi:10.1128/JB.00458-09

561 Bodelón G, Palomino C, Fernández LÁ. 2013. Immunoglobulin domains in *Escherichia coli* and
562 other enterobacteria: From pathogenesis to applications in antibody technologies. *FEMS*
563 *Microbiol Rev*. doi:10.1111/j.1574-6976.2012.00347.x

564 Buchy P, Ascioglu S, Buisson Y, Datta S, Nissen M, Tambyah PA, Vong S. 2020. Impact of vaccines
565 on antimicrobial resistance. *International Journal of Infectious Diseases*.
566 doi:10.1016/j.ijid.2019.10.005

567 Buckner MMC, Ciusa ML, Piddock LJV. 2018. Strategies to combat antimicrobial resistance: Anti-
568 plasmid and plasmid curing. *FEMS Microbiol Rev*. doi:10.1093/femsre/fuy031

569 Butler T, Shuster CW, Dixon P. 1981. Treatment of experimental *Salmonella* typhimurium
570 infection with mecillinam and ampicillin. *Antimicrob Agents Chemother* **19**:328–331.
571 doi:10.1128/AAC.19.2.328

572 Call DR, Singer RS, Meng D, Broschat SL, Orfe LH, Anderson JM, Herndon DR, Kappmeyer LS,
573 Daniels JB, Besser TE. 2010. blaCMY-2-positive IncA/C plasmids from *Escherichia coli* and
574 *Salmonella* enterica are a distinct component of a larger lineage of plasmids. *Antimicrob*
575 *Agents Chemother* **54**:590–596. doi:10.1128/AAC.00055-09

576 Carattoli A. 2013. Plasmids and the spread of resistance. *International Journal of Medical*
577 *Microbiology*. doi:10.1016/j.ijmm.2013.02.001

578 Carattoli A. 2009. Resistance plasmid families in Enterobacteriaceae. *Antimicrob Agents*
579 *Chemother*. doi:10.1128/AAC.01707-08

580 Casasnovas JM, Margolles Y, Noriega MA, Guzmán M, Arranz R, Melero R, Casanova M, Corbera
581 JA, Jiménez-de-Oya N, Gastaminza P, Garaigorta U, Saiz JC, Martín-Acebes MÁ, Fernández
582 LÁ. 2022. Nanobodies Protecting From Lethal SARS-CoV-2 Infection Target Receptor
583 Binding Epitopes Preserved in Virus Variants Other Than Omicron. *Front Immunol* **13**.
584 doi:10.3389/fimmu.2022.863831

585 Ciofu O, Bagge N, Høiby N. 2002. Antibodies against β-lactamase can improve ceftazidime
586 treatment of lung infection with β-lactam-resistant *Pseudomonas aeruginosa* in a rat
587 model of chronic lung infection. *APMIS* **110**:881–891. doi:10.1034/j.1600-
588 0463.2002.1101207.x

589 Cook MA, Wright GD. 2022. The past, present, and future of antibiotics. *Sci Transl Med* **14**:7793.
590 doi:10.1126/scitranslmed.abo7793

591 Datsenko KA, Wanner BL. 2000. One-step inactivation of chromosomal genes in *Escherichia coli*
592 K-12 using PCR products. *Proc Natl Acad Sci U S A* **97**:6640–6645.
593 doi:10.1073/pnas.120163297

594 Dolejska M, Villa L, Poirel L, Nordmann P, Carattoli A. 2013. Complete sequencing of an IncHI1
595 plasmid encoding the carbapenemase NDM-1, the ArmA 16s RNA methylase and a
596 resistance-nodulation-cell division/multidrug efflux pump. *Journal of Antimicrobial*
597 *Chemotherapy* **68**:34–39. doi:10.1093/jac/dks357

598 Eda R, Nakamura M, Takayama Y, Maehana S, Nakano R, Yano H, Kitasato H. 2020. Trends and
599 molecular characteristics of carbapenemase-producing Enterobacteriaceae in Japanese
600 hospital from 2006 to 2015. *Journal of Infection and Chemotherapy* **26**:667–671.
601 doi:10.1016/j.jiac.2020.02.002

602 Fairman JW, Dautin N, Wojtowicz D, Liu W, Noinaj N, Barnard TJ, Udho E, Przytycka TM, Cherezov
603 V, Buchanan SK. 2012. Crystal Structures of the Outer Membrane Domain of Intimin and
604 Invasin from Enterohemorrhagic *E. coli* and Enteropathogenic *Y. pseudotuberculosis*.
605 *Structure* **20**:1233–1243. doi:10.1016/j.str.2012.04.011

606 Fernández-Alarcón C, Singer RS, Johnson TJ. 2011. Comparative genomics of multidrug
607 resistance-encoding incA/C plasmids from commensal and pathogenic *Escherichia coli*
608 from multiple animal sources. *PLoS One* **6**. doi:10.1371/journal.pone.0023415

609 Forde BM, Zowawi HM, Harris PNA, Roberts L, Ibrahim E, Shaikh N, Deshmukh A, Sid Ahmed MA,
610 Al Maslamani M, Cottrell K, Trembizki E, Sundac L, Yu HH, Li J, Schembri MA, Whiley DM,
611 Paterson DL, Beatson SA. 2018. Discovery of *mcr-1* -Mediated Colistin Resistance in a Highly
612 Virulent *Escherichia coli* Lineage. *mSphere* **3**. doi:10.1128/mSphere.00486-18

613 Fricke WF, Welch TJ, McDermott PF, Mammel MK, LeClerc JE, White DG, Cebula TA, Ravel J.
614 2009. Comparative genomics of the IncA/C multidrug resistance plasmid family. *J Bacteriol*
615 **191**:4750–4757. doi:10.1128/JB.00189-09

616 Frost I, Balachandran A, Paulin-Deschenaux S, Sati H, Hasso-Agopsowicz M. 2022. The approach
617 of World Health Organization to articulate the role and assure impact of vaccines against
618 antimicrobial resistance. *Hum Vaccin Immunother*. doi:10.1080/21645515.2022.2145069

619 Garcia-Just A, Miró L, Pérez-Bosque A, Amat C, Polo J, Pallàs M, Griñán-Ferré C, Moretó M. 2020.
620 Dietary spray-dried porcine plasma prevents cognitive decline in senescent mice and
621 reduces neuroinflammation and oxidative stress. *Journal of Nutrition* **150**:303–311.
622 doi:10.1093/jn/nxz239

623 Glass DS, Riedel-Kruse IH. 2018. A Synthetic Bacterial Cell-Cell Adhesion Toolbox for
624 Programming Multicellular Morphologies and Patterns. *Cell* **174**:649-658.e16.
625 doi:10.1016/j.cell.2018.06.041

626 Graf FE, Palm M, Warringer J, Farewell A. 2019. Inhibiting conjugation as a tool in the fight
627 against antibiotic resistance. *Drug Dev Res* **80**:19–23. doi:10.1002/ddr.21457

628 Hamers-Casterman C, Atarhouch T, Muyldermans S, Robinson G, Hammers C, Songa EB,
629 Bendahman N, Hammers R. 1993. Naturally occurring antibodies devoid of light chains.
630 *Nature* **363**:446–448. doi:10.1038/363446a0

631 Holt KE, Phan MD, Baker S, Duy PT, Nga TVT, Nair S, Turner AK, Walsh C, Fanning S, Farrell-Ward
632 S, Dutta S, Kariuki S, WeillFranç FX, Parkhill J, Dougan G, Wain J. 2011. Emergence of a
633 globally dominant inchi1 plasmid type associated with multiple drug resistant typhoid.
634 *PLoS Negl Trop Dis* **5**. doi:10.1371/journal.pntd.0001245

635 Hüttener M, Hergueta J, Bernabeu M, Prieto A, Aznar S, Merino S, Tomás J, Juárez A. 2022. Roles
636 of Proteins Containing Immunoglobulin-Like Domains in the Conjugation of Bacterial
637 Plasmids. *mSphere* **7**. doi:10.1128/msphere.00978-21

638 Hüttener M, Prieto A, Aznar S, Bernabeu M, Glaría E, Valledor AF, Paytubi S, Merino S, Tomás J,
639 Juárez A. 2019. Expression of a novel class of bacterial Ig-like proteins is required for IncHI
640 plasmid conjugation. *PLoS Genet* **15**. doi:10.1371/journal.pgen.1008399

641 Ingle DJ, Ambrose RL, Baines SL, Duchene S, Gonçalves da Silva A, Lee DYJ, Jones M, Valcanis M,
642 Taiaroa G, Ballard SA, Kirk MD, Howden BP, Pearson JS, Williamson DA. 2021. Evolutionary
643 dynamics of multidrug resistant *Salmonella enterica* serovar 4,[5],12:i:- in Australia. *Nat*
644 *Commun* **12**. doi:10.1038/s41467-021-25073-w

645 Jovčevska I, Muyldermans S. 2020. The Therapeutic Potential of Nanobodies. *BioDrugs* **34**:11–
646 26. doi:10.1007/s40259-019-00392-z

647 Khanum S, Carbone V, Gupta SK, Yeung J, Shu D, Wilson T, Parlane NA, Altermann E, Estein SM,
648 Janssen PH, Wedlock DN, Heiser A. 2022. Mapping immunogenic epitopes of an adhesin-
649 like protein from Methanobrevibacter ruminantium M1 and comparison of empirical data
650 with in silico prediction methods. *Sci Rep* **12**:10394. doi:10.1038/s41598-022-14545-8

651 Koizumi N, Watanabe H. 2004. Leptospiral immunoglobulin-like proteins elicit protective
652 immunity. *Vaccine* **22**:1545–1552. doi:10.1016/j.vaccine.2003.10.007

653 Lawley TD, Gilmour MW, Gunton JE, Standeven LJ, Taylor DE. 2002. Functional and mutational
654 analysis of conjugative transfer region 1 (Tra1) from the IncHI1 plasmid R27. *J Bacteriol*
655 **184**:2173–2180. doi:10.1128/JB.184.8.2173-2180.2002

656 Lawley TD, Gilmour MW, Gunton JE, Tracz DM, Taylor DE. 2003. Functional and mutational
657 analysis of conjugative transfer region 2 (Tra2) from the IncHI1 plasmid R27. *J Bacteriol*
658 **185**:581–591. doi:10.1128/JB.185.2.581-591.2003

659 Lim LM, Ly N, Anderson D, Yang JC, Macander L, Jarkowski A, Forrest A, Bulitta JB, Tsuji BT. 2010.
660 Resurgence of colistin: A review of resistance, toxicity, pharmacodynamics, and dosing.
661 *Pharmacotherapy*. doi:10.1592/phco.30.12.1279

662 Lipsitch M, Siber GR. 2016. How can vaccines contribute to solving the antimicrobial resistance
663 problem? *mBio*. doi:10.1128/mBio.00428-16

664 Matamoros S, Van Hattem JM, Arcilla MS, Willemse N, Melles DC, Penders J, Vinh TN, Thi Hoa
665 N, Bootsma MCJ, Van Genderen PJ, Goorhuis A, Grobusch M, Molhoek N, Oude Lashof
666 AML, Stobberingh EE, Verbrugh HA, De Jong MD, Schultsz C. 2017. Global phylogenetic
667 analysis of *Escherichia coli* and plasmids carrying the mcr-1 gene indicates bacterial
668 diversity but plasmid restriction. *Sci Rep* **7**. doi:10.1038/s41598-017-15539-7

669 Meyer E, Schwab F, Schroeren-Boersch B, Gastmeier P. 2010. Dramatic increase of third-
670 generation cephalosporin-resistant *E. coli* in German intensive care units: Secular trends in
671 antibiotic drug use and bacterial resistance, 2001 to 2008. *Crit Care* **14**. doi:10.1186/cc9062

672 Micoli F, Bagnoli F, Rappuoli R, Serruto D. 2021. The role of vaccines in combatting antimicrobial
673 resistance. *Nat Rev Microbiol* **19**:287–302. doi:10.1038/s41579-020-00506-3

674 Miró L, Rosell-Cardona C, Amat C, Polo J, Moretó M, Pérez-Bosque A. 2023. Dietary
675 supplementation with spray-dried animal plasma improves vaccine protection in aged
676 mice. *Front Nutr* **10**. doi:10.3389/fnut.2023.1050961

677 Morens DM, Folkers GK, Fauci AS. 2004. The challenge of emerging and re-emerging infectious
678 diseases. *Nature* **430**:242–249. doi:10.1038/nature02759

679 Moriel DG, Bertoldi I, Spagnuolo A, Marchi S, Rosini R, Nesta B, Pastorello I, Corea VAM, Torricelli
680 G, Cartocci E, Savino S, Scarselli M, Dobrindt U, Hacker J, Tettelin H, Tallon LJ, Sullivan S,
681 Wieler LH, Ewers C, Pickard D, Dougan G, Fontana MR, Rappuoli R, Pizza M, Serino L. 2010.
682 Identification of protective and broadly conserved vaccine antigens from the genome of
683 extraintestinal pathogenic *Escherichia coli*. *Proceedings of the National Academy of*
684 *Sciences* **107**:9072–9077. doi:10.1073/pnas.0915077107

685 Murray CJ, Ikuta KS, Sharara F, Swetschinski L, Robles Aguilar G, Gray A, Han C, Bisignano C, Rao
686 P, Wool E, Johnson SC, Browne AJ, Chipeta MG, Fell F, Hackett S, Haines-Woodhouse G,
687 Kashef Hamadani BH, Kumaran EAP, McManigal B, Agarwal R, Akech S, Albertson S, Amuasi
688 J, Andrews J, Aravkin A, Ashley E, Bailey F, Baker S, Basnyat B, Bekker A, Bender R, Bethou
689 A, Bielicki J, Boonkasidecha S, Bukosia J, Carvalheiro C, Castañeda-Orjuela C, Chansamouth
690 V, Chaurasia S, Chiurchiù S, Chowdhury F, Cook AJ, Cooper B, Cressey TR, Criollo-Mora E,
691 Cunningham M, Darboe S, Day NPJ, De Luca M, Dokova K, Dramowski A, Dunachie SJ,
692 Eckmanns T, Eibach D, Emami A, Feasey N, Fisher-Pearson N, Forrest K, Garrett D,
693 Gastmeier P, Giref AZ, Greer RC, Gupta V, Haller S, Haselbeck A, Hay SI, Holm M, Hopkins

694 S, Iregbu KC, Jacobs J, Jarovsky D, Javanmardi F, Khorana M, Kissoon N, Kobeissi E,
695 Kostyanev T, Krapp F, Krumkamp R, Kumar A, Kyu HH, Lim C, Limmathurotsakul D, Loftus
696 MJ, Lunn M, Ma J, Mturi N, Munera-Huertas T, Musicha P, Mussi-Pinhata MM, Nakamura
697 T, Nanavati R, Nangia S, Newton P, Ngoun C, Novotney A, Nwakanma D, Obiero CW, Olivas-
698 Martinez A, Olliaro P, Ooko E, Ortiz-Brizuela E, Peleg AY, Perrone C, Plakkal N, Ponce-de-
699 Leon A, Raad M, Ramdin T, Riddell A, Roberts T, Robotham JV, Roca A, Rudd KE, Russell N,
700 Schnall J, Scott JAG, Shivamallappa M, Sifuentes-Osornio J, Steenkeste N, Stewardson AJ,
701 Stoeva T, Tasak N, Thaiprakong A, Thwaites G, Turner C, Turner P, van Doorn HR, Velaphi
702 S, Vongpradith A, Vu H, Walsh T, Waner S, Wangrangsimakul T, Wozniak T, Zheng P,
703 Sartorius B, Lopez AD, Stergachis A, Moore C, Dolecek C, Naghavi M. 2022. Global burden
704 of bacterial antimicrobial resistance in 2019: a systematic analysis. *The Lancet* **399**:629–
705 655. doi:10.1016/S0140-6736(21)02724-0

706 Muyldermans S. 2021. Applications of Nanobodies. *Annu Rev Anim Biosci* **9**:401–421.
707 doi:10.1146/annurev-animal-021419-083831

708 Muyldermans S. 2013. Nanobodies: Natural single-domain antibodies. *Annu Rev Biochem*.
709 doi:10.1146/annurev-biochem-063011-092449

710 Nesta B, Spraggon G, Alteri C, Moriel DG, Rosini R, Veggi D, Smith S, Bertoldi I, Pastorello I,
711 Ferlenghi I, Fontana MR, Frankel G, Mobley HLT, Rappuoli R, Pizza M, Serino L, Soriani M.
712 2012. FdeC, a novel broadly conserved *Escherichia coli* adhesin eliciting protection against
713 urinary tract infections. *mBio* **3**. doi:10.1128/mBio.00010-12

714 Novick RP, Richmond MH. 1965. Nature and Interactions of the Genetic Elements Governing
715 Penicillinase Synthesis in *Staphylococcus aureus*. *J Bacteriol* **90**:467–480.
716 doi:10.1128/jb.90.2.467-480.1965

717 Parvez S, Khan AU. 2018. Hospital sewage water: a reservoir for variants of New Delhi metallo-
718 β-lactamase (NDM)- and extended-spectrum β-lactamase (ESBL)-producing
719 Enterobacteriaceae. *Int J Antimicrob Agents* **51**:82–88.
720 doi:10.1016/j.ijantimicag.2017.08.032

721 Phan M-D, Wain J. 2008. IncHI plasmids, a dynamic link between resistance and pathogenicity.
722 *The Journal of Infection in Developing Countries* **2**. doi:10.3855/jidc.221

723 Piñero-Lambea C, Bodelón G, Fernández-Periáñez R, Cuesta AM, Álvarez-Vallina L, Fernández LÁ.
724 2015. Programming Controlled Adhesion of *E. coli* to Target Surfaces, Cells, and Tumors
725 with Synthetic Adhesins. *ACS Synth Biol* **4**:463–473. doi:10.1021/sb500252a

726 Qamar MU, Ejaz H, Walsh TR, Shah AA, Al Farraj DA, Alkufeidy RM, Alkubaisi NA, Saleem S, Jahan
727 S. 2021. Clonal relatedness and plasmid profiling of extensively drug-resistant New Delhi
728 metallo-β-lactamase-producing *Klebsiella pneumoniae* clinical isolates. *Future Microbiol*
729 **16**:229–239. doi:10.2217/fmb-2020-0315

730 Ren W, Yin J, Duan J, Liu G, Zhu X, Chen S, Li T, Wang S, Tang Y, Hardwidge PR. 2014. Mouse
731 intestinal innate immune responses altered by enterotoxigenic *Escherichia coli* (ETEC)
732 infection. *Microbes Infect* **16**:954–961. doi:10.1016/j.micinf.2014.09.005

733 Robledo M, Álvarez B, Cuevas A, González S, Ruano-Gallego D, Fernández LÁ, de la Cruz F. 2022.
734 Targeted bacterial conjugation mediated by synthetic cell-to-cell adhesions. *Nucleic Acids*
735 *Res* **50**:12938–12950. doi:10.1093/nar/gkac1164

736 Rosell-Cardona C, Amat C, Griñán-Ferré C, Polo J, Pallàs M, Pérez-Bosque A, Moretó M, Miró L.
737 2022. The Neuroprotective Effects of Spray-Dried Porcine Plasma Supplementation Involve
738 the Microbiota−Gut−Brain Axis. *Nutrients* **14**. doi:10.3390/nu14112211

739 Rossi O, Dybowski R, Maskell DJ, Grant AJ, Restif O, Mastroeni P. 2017. Within-host
740 spatiotemporal dynamics of systemic *Salmonella* infection during and after antimicrobial
741 treatment. *Journal of Antimicrobial Chemotherapy* **72**:3390–3397. doi:10.1093/jac/dkx294

742 Rossolini GM, Mantengoli E, Docquier J-D, Musmanno RA, Coratza G. 2007. Epidemiology of
743 infections caused by multiresistant gram-negatives: ESBLs, MBLs, panresistant strains. *New*
744 *Microbiol* **30**:332–9.

745 Rozwandowicz M, Brouwer MSM, Fischer J, Wagenaar JA, Gonzalez-Zorn B, Guerra B, Mevius DJ,
746 Hordijk J. 2018. Plasmids carrying antimicrobial resistance genes in Enterobacteriaceae.
747 *Journal of Antimicrobial Chemotherapy* **73**:1121–1137. doi:10.1093/jac/dkx488

748 Salema V, Fernández LÁ. 2017. *Escherichia* coli surface display for the selection of nanobodies.
749 *Microb Biotechnol* **10**:1468–1484. doi:10.1111/1751-7915.12819

750 Salema V, López-Guajardo A, Gutierrez C, Mencía M, Fernández LÁ. 2016. Characterization of
751 nanobodies binding human fibrinogen selected by *E. coli* display. *J Biotechnol* **234**:58–65.
752 doi:10.1016/j.jbiotec.2016.07.025

753 Salema V, Marín E, Martínez-Arteaga R, Ruano-Gallego D, Fraile S, Margolles Y, Teira X, Gutierrez
754 C, Bodelón G, Fernández LÁ. 2013. Selection of Single Domain Antibodies from Immune
755 Libraries Displayed on the Surface of *E. coli* Cells with Two β-Domains of Opposite
756 Topologies. *PLoS One* **8**:e75126. doi:10.1371/journal.pone.0075126

757 Schmittgen TD, Livak KJ. 2008. Analyzing real-time PCR data by the comparative CT method. *Nat*
758 *Protoc* **3**:1101–1108. doi:10.1038/nprot.2008.73

759 Senna JPM, Roth DM, Oliveira JS, Machado DC, Santos DS. 2003. Protective immune response
760 against methicillin resistant *Staphylococcus aureus* in a murine model using a DNA vaccine
761 approach. *Vaccine* **21**:2661–2666. doi:10.1016/S0264-410X(02)00738-7

762 Sherburne CK, Lawley TD, Gilmour MW, Blattner FR, Burland V, Grotbeck E, Rose DJ, Taylor DE.
763 2000. The complete DNA sequence and analysis of R27, a large IncHI plasmid from
764 *Salmonella* typhi that is temperature sensitive for transfer. *Nucleic Acids Res* **28**:2177–86.
765 doi:10.1093/nar/28.10.2177

766 Spellberg B, Guidos R, Gilbert D, Bradley J, Boucher HW, Scheld WM, Bartlett JG, Edwards J.
767 2008. The epidemic of antibiotic-resistant infections: A call to action for the medical
768 community from the infectious diseases society of America. *Clinical Infectious Diseases*.
769 doi:10.1086/524891

770 Suzuki H, Yano H, Brown CJ, Top EM. 2010. Predicting plasmid promiscuity based on genomic
771 signature. *J Bacteriol* **192**:6045–6055. doi:10.1128/JB.00277-10

772 Tanmoy AM, Westeel E, De Bruyne K, Goris J, Rajoharison A, Sajib MSI, Van Belkum A, Saha SK,
773 Komurian-Pradel F, Endtz HP. 2018. *Salmonella enterica* Serovar Typhi in Bangladesh:
774 Exploration of Genomic Diversity and Antimicrobial Resistance. doi:10.1128/mBio.00105

775 Thomas CM, Nielsen KM. 2005. Mechanisms of, and barriers to, horizontal gene transfer
776 between bacteria. *Nat Rev Microbiol*. doi:10.1038/nrmicro1234

Tiller T, Meffre E, Yurasov S, Tsuiji M, Nussenzweig MC, Wardemann H. 2008. Efficient generation of monoclonal antibodies from single human B cells by single cell RT-PCR and expression vector cloning. *J Immunol Methods* **329**:112–124. doi:10.1016/j.jim.2007.09.017

Troisi M, Andreano E, Sala C, Kabanova A, Rappuoli R. 2020. Vaccines as remedy for antimicrobial resistance and emerging infections. *Curr Opin Immunol*. doi:10.1016/j.coi.2020.09.003

Villa L, Poirel L, Nordmann P, Carta C, Carattoli A. 2012. Complete sequencing of an IncH plasmid carrying the bla ndm-1, bla ctx-m-15 and qnrB1 genes. *Journal of Antimicrobial Chemotherapy* **67**:1645–1650. doi:10.1093/jac/dks114

Vrancianu CO, Popa LI, Bleotu C, Chifiriuc MC. 2020. Targeting Plasmids to Limit Acquisition and Transmission of Antimicrobial Resistance. *Front Microbiol*. doi:10.3389/fmicb.2020.00761

Wang J, Stephan R, Zurfluh K, Hächler H, Fanning S. 2015. Characterization of the genetic environment of blaESBL genes, integrons and toxin-antitoxin systems identified on large transferrable plasmids in multi-drug resistant *Escherichia coli*. *Front Microbiol* **6**. doi:10.3389/fmicb.2014.00716

Wang Y, Tian GB, Zhang R, Shen Y, Tyrrell JM, Huang X, Zhou H, Lei L, Li HY, Doi Y, Fang Y, Ren H, Zhong LL, Shen Z, Zeng KJ, Wang S, Liu JH, Wu C, Walsh TR, Shen J. 2017. Prevalence, risk factors, outcomes, and molecular epidemiology of mcr-1-positive Enterobacteriaceae in patients and healthy adults from China: an epidemiological and clinical study. *Lancet Infect Dis* **17**:390–399. doi:10.1016/S1473-3099(16)30527-8

Welch TJ, Fricke WF, McDermott PF, White DG, Rosso ML, Rasko DA, Mammel MK, Eppinger M, Rosovitz MJ, Wagner D, Rahalison L, LeClerc JE, Hinshaw JM, Lindler LE, Cebula TA, Carniel E, Ravel J. 2007. Multiple antimicrobial resistance in plague: An emerging public health risk. *PLoS One* **2**. doi:10.1371/journal.pone.0000309

World Health Organization. 2019. Typhoid vaccines: WHO position paper, March 2018 – Recommendations. *Vaccine* **37**:214–216. doi:10.1016/j.vaccine.2018.04.022

Yuki Y, Zuo F, Kurokawa S, Uchida Y, Sato S, Sakon N, Hammarström L, Kiyono H, Marcotte H. 2023. Lactobacilli as a Vector for Delivery of Nanobodies against Norovirus Infection. *Pharmaceutics* **15**. doi:10.3390/pharmaceutics15010063

Zarantonelli ML, Antignac A, Lancellotti M, Guiyoule A, Alonso JM, Taha MK. 2006. Immunogenicity of meningococcal PBP2 during natural infection and protective activity of anti-PBP2 antibodies against meningococcal bacteraemia in mice. *Journal of Antimicrobial Chemotherapy* **57**:924–930. doi:10.1093/jac/dkl066

Zhang Zhiren, Guo H, Li Xiaodong, Li W, Yang G, Ni W, Zhan M, Lu L, Zhang Zhenlin, Li Xiaobin, Zhou Z. 2021. Genetic Diversity and Characteristics of blaNDM-Positive Plasmids in *Escherichia coli*. *Front Microbiol* **12**. doi:10.3389/fmicb.2021.729952

Zheng B, Dong H, Xu H, Lv J, Zhang J, Jiang X, Du Y, Xiao Y, Li L. 2016. Coexistence of MCR-1 and NDM-1 in Clinical *Escherichia coli* Isolates. *Clinical Infectious Diseases*. doi:10.1093/cid/ciw553

Acknowledgments

This work was supported by grants from Fundació “La Marató TV3,” Spain (project 201818 10), CERCA Program/Generalitat de Catalunya to AJ, PID2021-124676NB-I00 from the Ministerio de Economía, Industria y Competitividad to SM and JT. Work in the laboratory of LAF is supported by grants PLEC2021-007739 from MCIN/AEI NextGeneration EU/ PRTR and FET Open 965018-BIOCELLPHE from the European Union’s Horizon 2020 Future and Emerging Technologies research and innovation program. LM and APB are members of the Institut de Recerca en Nutrició, i Seguretat Alimentària (INSA-UB), which is recognized as a Maria de Maeztu Unit of Excellence and funded by MICIN/AEI/FEDER (CEX2021-001234-M).

Contributions

Genetic manipulations, conjugative transfer of the RSP plasmid and purification of the variants of the RSP protein were conducted by A. Prieto, M. Hüttener, D. Salguero and M. Bernabeu. *In vivo* experiments with mice were conducted by L. Miró and A. Pérez-Bosque. Electron microscopy studies were conducted by S. Merino and J. Tomás. Selection of clones producing anti-RSP nanobodies and the analysis of the effect of the obtained nanobodies on the conjugative transfer of the RSP plasmid were performed by Y. Margolles, L.A. Fernández and A. Prieto. The initial manuscript draft was written by A. Prieto, A. Pérez-Bosque and A. Juárez. A. Prieto, A. Pérez-Bosque, L.A. Fernández, M. Hüttener, and A. Juárez edited the final version. A. Juárez was the PI of the project.

Ethics

The dromedary camel immunization protocol followed European Union and Spanish guidelines of animal experimentation and was approved by the Ethics Committee for Animal Experimentation from University of Las Palmas de Gran Canaria and the Consejería de Agricultura, Pesca y Aguas of the Canary Islands Goverment (reference OEBA_ULPGC_20-2023). Experimentation with mice was conducted at Animal Facility of Faculty of Pharmacy and Food

843 Science. Experiments were approved by the Ethics Committee of Animal Experimentation of the
844 University of Barcelona (Ref. 170/20). Animals were handled in strict accordance with the
845 guidelines of the European Community 86/609/CEE.

846 **Competing interests**

847 The authors declare no competing interests.

848

849 **Figures**

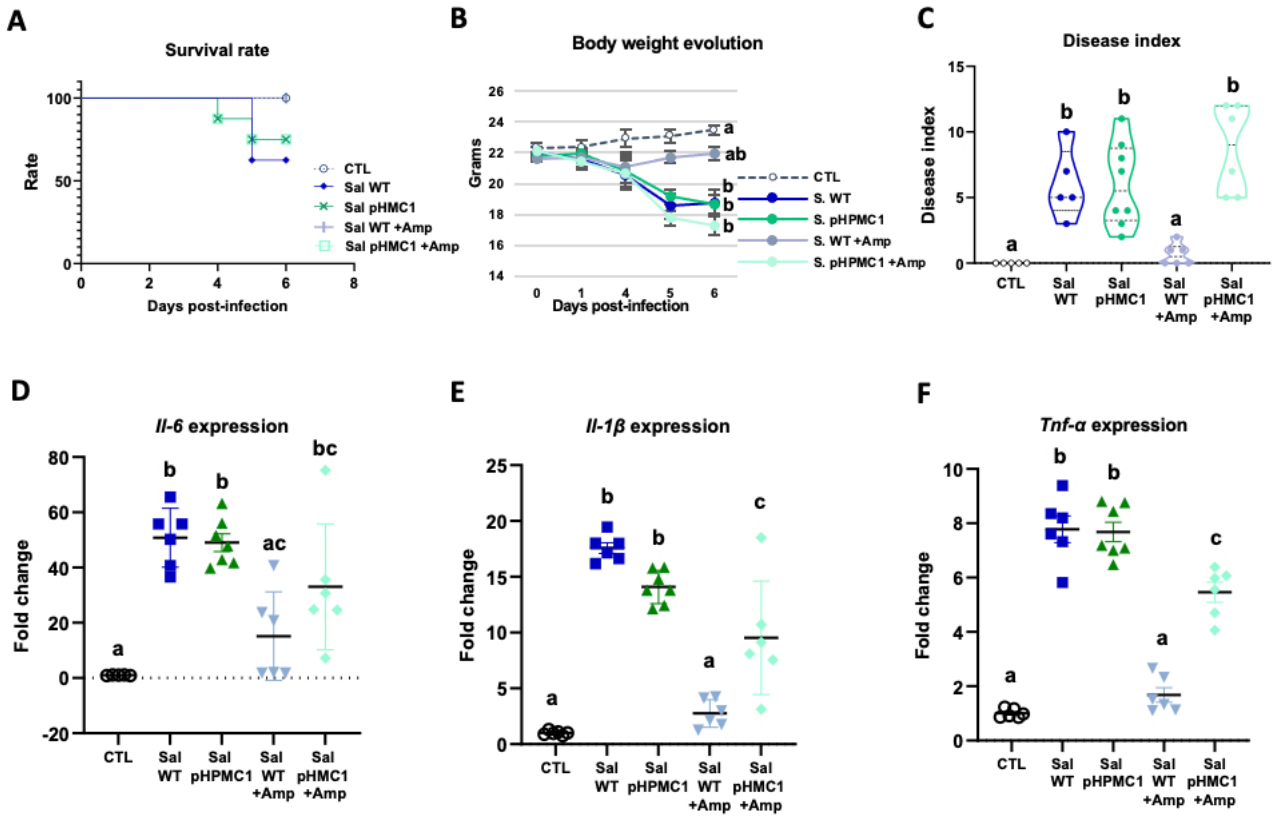

850

851 **Figure 1. Infection of mice with the *S.* Typhimurium SL1344 and *S.* Typhimurium (pHCM1)**
852 **strains.** Survival rate **(A)**, body weight evolution **(B)**, disease index **(C)** and proinflammatory
853 cytokine expression in spleen, *Il-6* **(D)**, *Il-1β* **(E)** and *Tnf-α* **(F)**. Groups treated with ampicillin
854 (Amp) are indicated with **+Amp**. In panel (A), survival rate of control animals and those infected
855 with the *S.* Typhimurium SL1344 (WT) strain and treated with Amp, are 100%. Animals infected
856 with the *S.* Typhimurium (pHCM1) strain have the same survival rate independently of the
857 treatment with Amp. Results are expressed as mean ± SEM (n= 6-8 animals). Means without a
858 common letter differ, P<0.05.

859

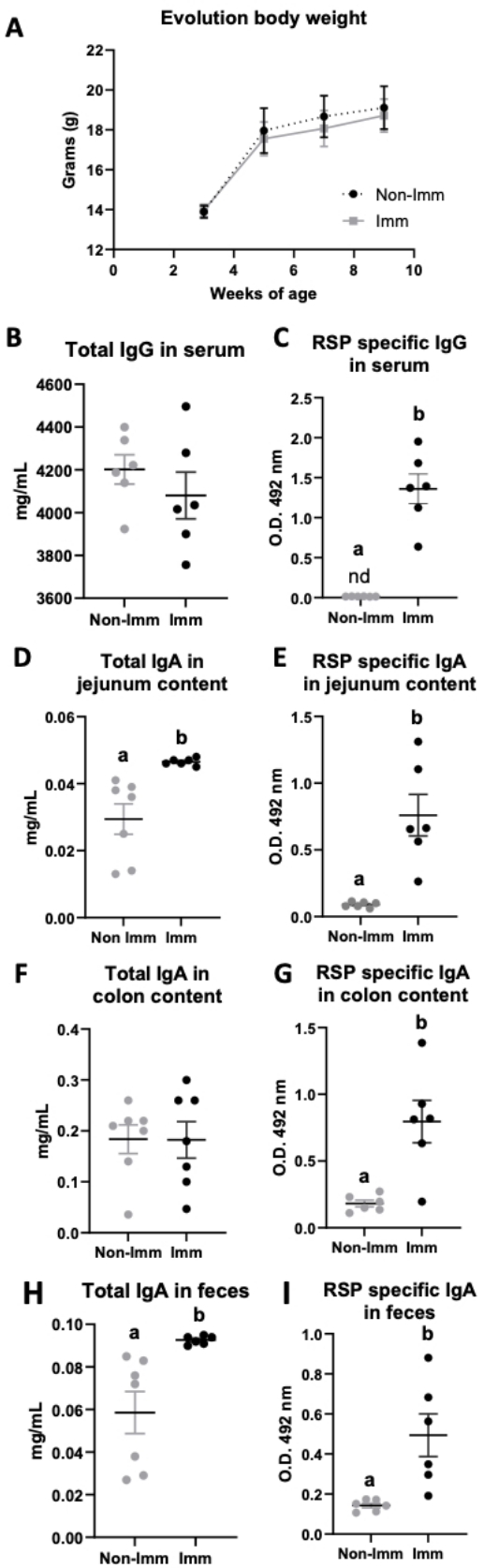
A
Evolution body weight
Grams (g)
Weeks of age
Non-Imm
Imm
B
Total IgG in serum
mg/mL
Non-Imm
Imm
C
RSP specific IgG in serum
O.D. 492 nm
a
b
nd
D
Total IgA in jejunum content
E
RSP specific IgA in jejunum content
F
Total IgA in colon content
G
RSP specific IgA in colon content
H
Total IgA in feces
I
RSP specific IgA in feces

860

861

862 **Figure 2. Effect of immunization with the RSP protein on body weight evolution (A) and**
863 **immunoglobulin concentration (B-I).** Open bars represent non-immunized (**No-Imm**) mice;
864 solid bars represent immunized (**Imm**) mice. Results are expressed as mean ± SEM (n= 6-8
865 animals). IgA, immunoglobulin A; IgG, immunoglobulin G; nd, non-detected. Means without a
866 common letter differ, $P<0.05$.

867

868

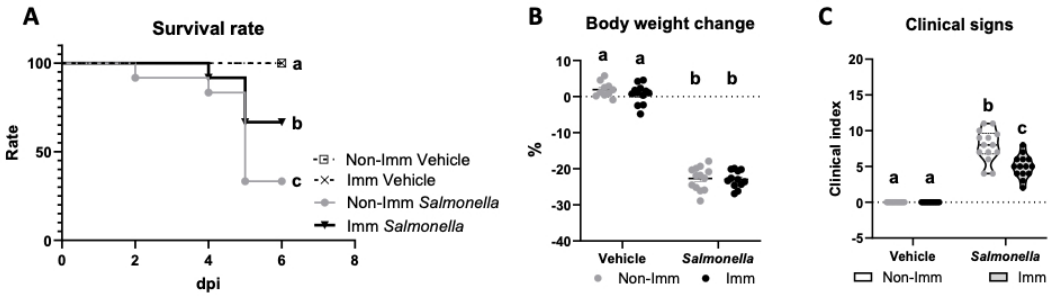

869

870 **Figure 3. Survival rate (A), body weight change (B) and clinical signs (C) after challenge with**

871 **the SL1344 (pHCM1) strain.** Open bars/plots represent non-immunized (**No-Imm**) mice; solid

872 bars/plots represent immunized (**Imm**) mice. In panel B, results are expressed as mean ± SEM

873 (n= 12-14 animals). Means without a common letter differ, P<0.05.

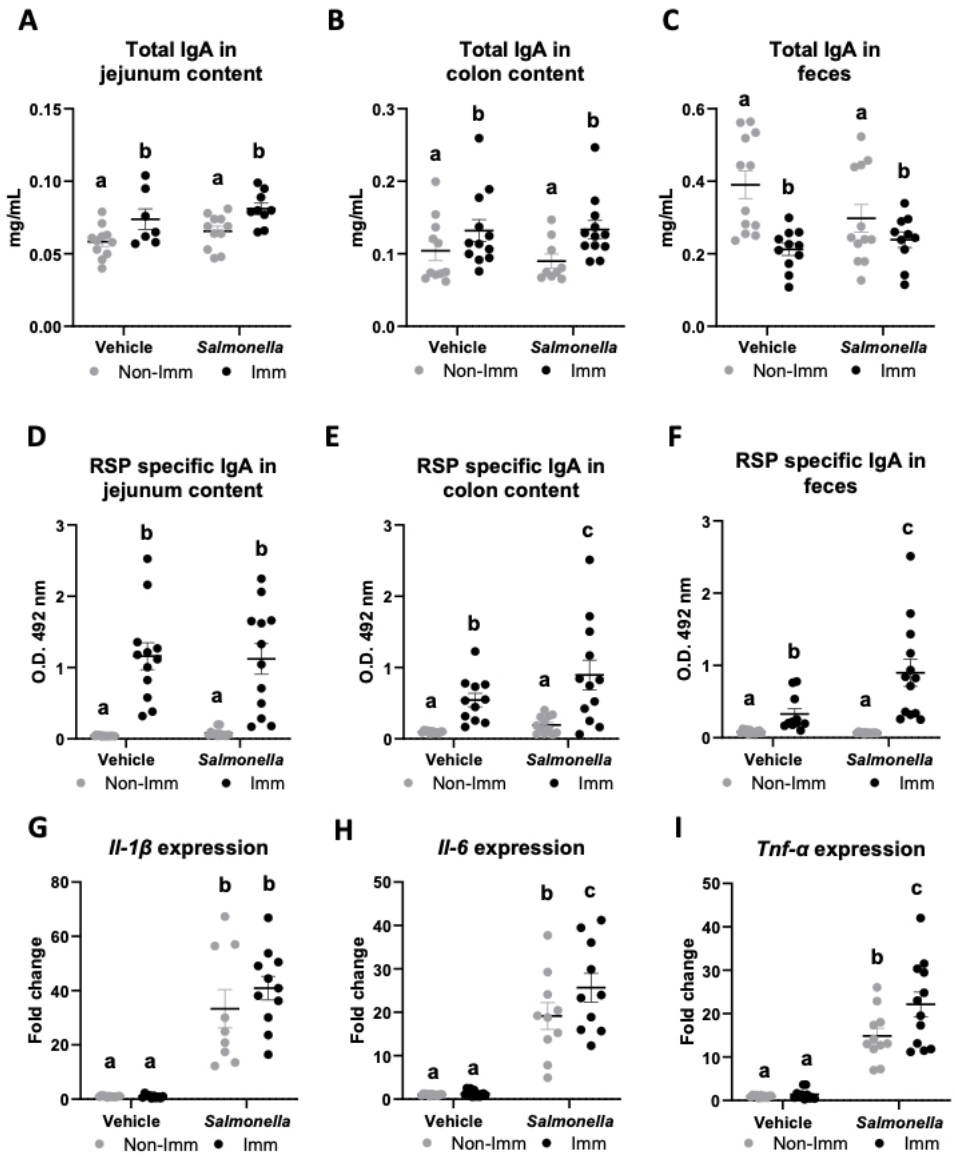

Figure 4. Immunoglobulin concentration and cytokine expression in the gastrointestinal tract after RSP immunization and challenge with *Salmonella.* Total IgA concentration in jejunum content **(A)**, in colon content **(B)** and in feces **(C)**. RSP-specific IgA titers in jejunum content **(D)**, in colon content **(E)** and in feces **(F)**. *Il-1β* **(G)**, *Il-6* **(H)** and *Tnf-α* **(I)** expression in colon mucosa. Open bars represent non-immunized (**Non-Imm**) mice; solid bars represent immunized (**Imm**) mice. Results are expressed as means ± SEMs (n= 10–12 animals). Means without a common letter differ, P<0.05. IgA, immunoglobulin A; IgG, immunoglobulin G; Il, interleukin; Int, interaction between both factors; Tnf-α, tumor necrosis factor alpha.

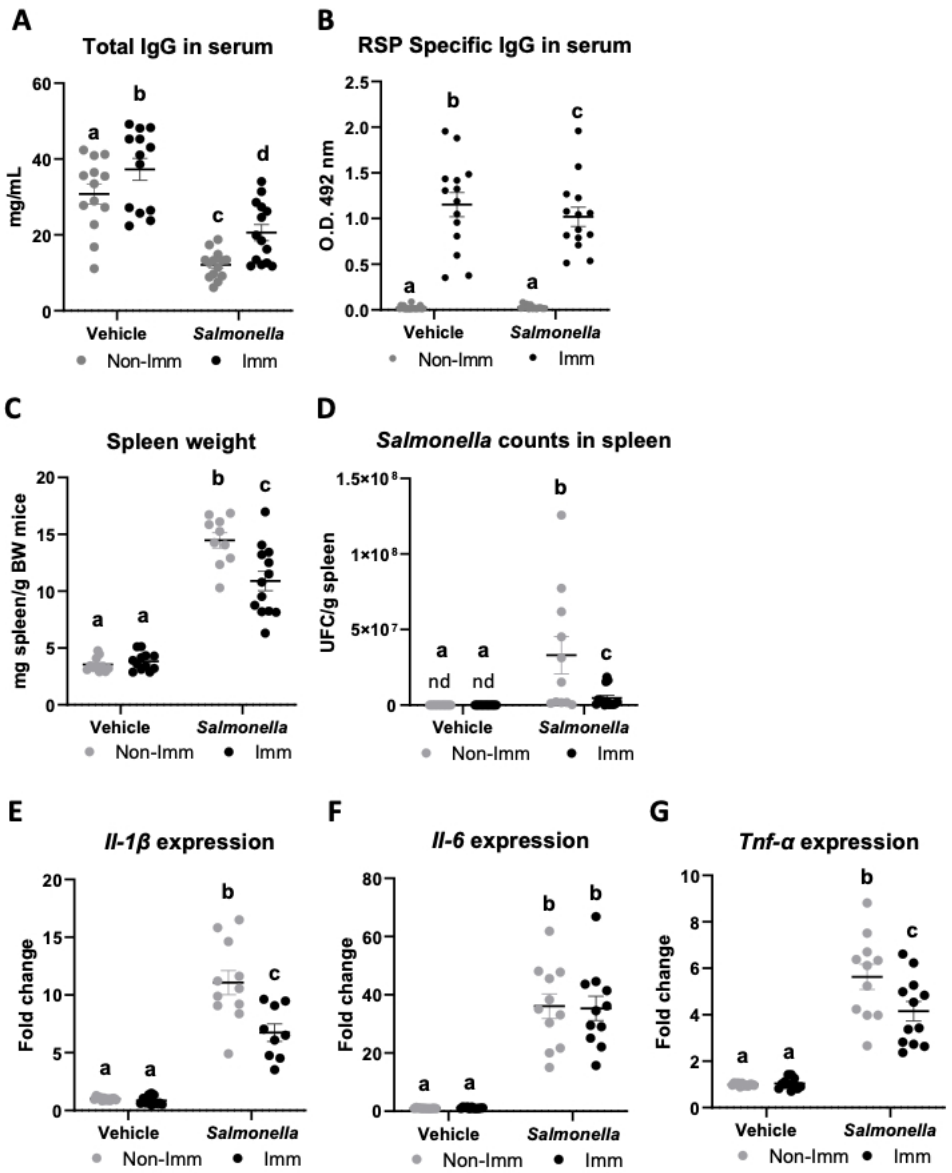

883

884 **Figure 5. Immunoglobulin concentration, spleen weight, *Salmonella* counts in spleen tissue**
885 **and cytokine expression in spleen tissue after immunization with the RSP protein and**
886 **challenge with the SL1344 (pHCM1) strain.** Total IgG concentration **(A)** and RSP-specific IgG
887 titers **(B)** in plasma. Spleen weight **(C)** and *Salmonella* counts in spleen tissue **(D)**. *Il-1β* **(E)**, *Il-6*
888 **(F)** and *Tnf-α* **(G)** expression in spleen tissue. Results are expressed as means ± SEMs (n= 12-14
889 animals). Means without a common letter differ, P<0.05. IgA, immunoglobulin A; IgG,
890 immunoglobulin G; Il, interleukin; nd, non-detected; Tnf-α, tumor necrosis factor alpha.

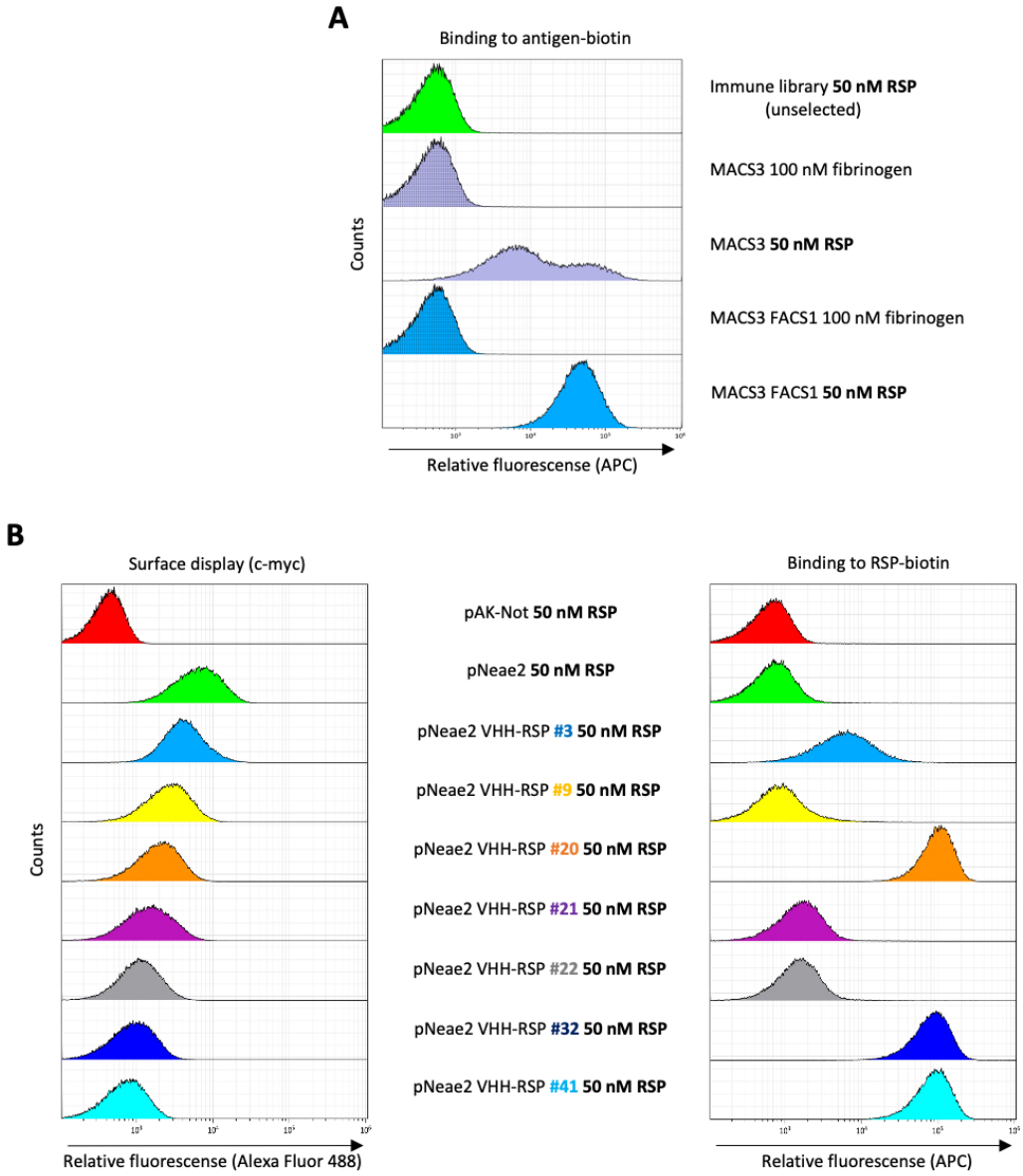

Figure 6. Selection of RSP-binding Nbs from immune libraries displayed on the surface of *E. coli.* (A) Flow cytometry analysis of the enrichment of bacterial population displaying Nb libraries generated after the immunization of dromedaries with the C-terminal domain of the RSP protein. 3 rounds of selection with the RSP protein by magnetic cell sorting (MACS) and one round of fluorescence activated cell sorting (FACS) were performed, in which bacteria were incubated with 50 nM of biotin-labeled RSP (or 100 nM of fibrinogen used as a specificity control) and stained with Streptavidin-APC. **(B)** Flow cytometry of the individual bacterial clones selected from the immune library. The bacterial surface display of the corresponding nanobody was

900 detected using an anti-c-myc monoclonal antibody. The binding of biotin-labeled antigens to
901 Nbs displayed on bacteria was performed with the incubation of bacterial cells with 50 nM of
902 biotin-labeled RSP.

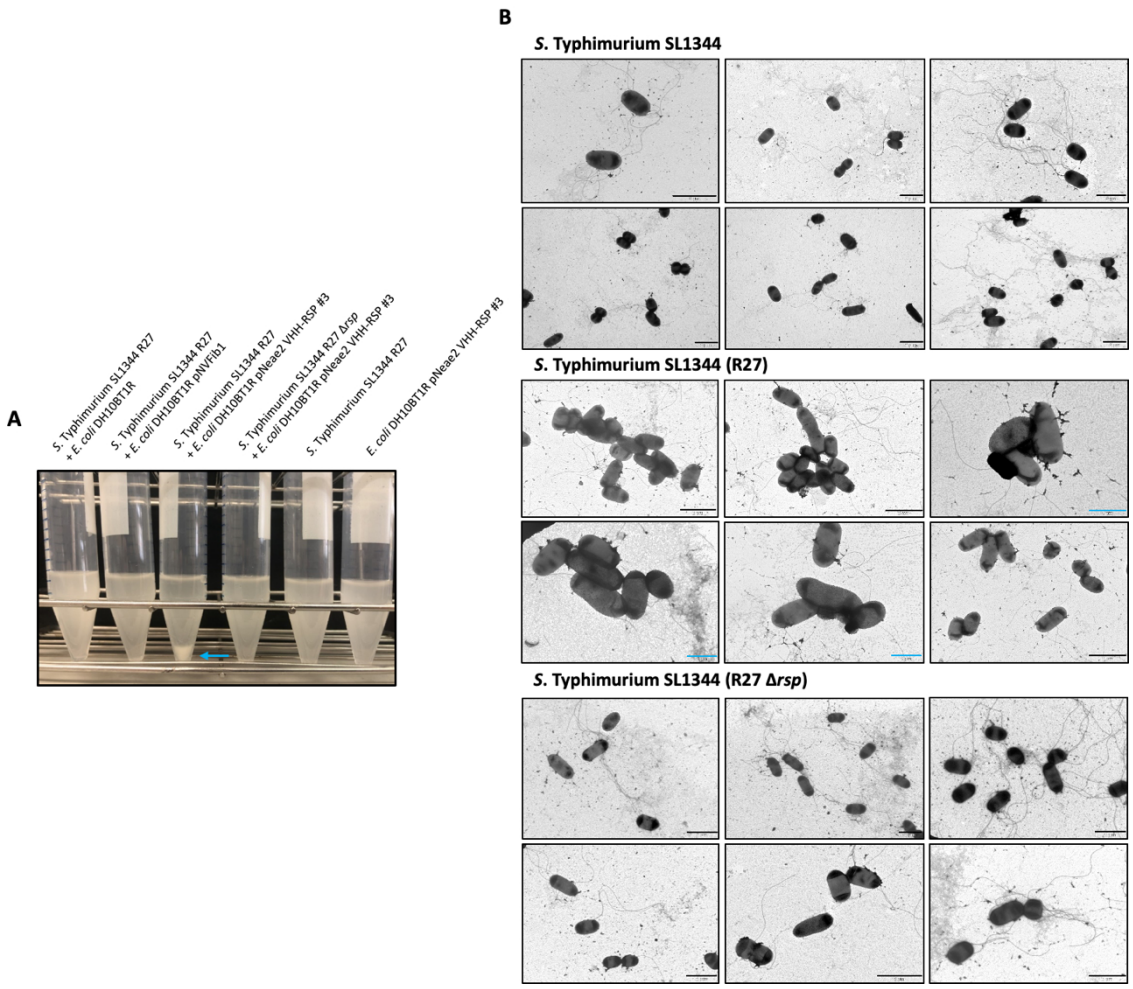

Figure 7. Analysis of the interaction of the VHH-RSP#3 isolated in the immune library with the native RSP protein at a macro and microscopic level. (A) Assay of the ability of *E. coli* DH10BT1R cells expressing nanobodies on its surface to agglutinate cells of the *S*. Typhimurium SL1344 (R27) strain. Blue arrow marks the aggregation of bacteria after the interaction of *E. coli* cells producing nanobodies directed against the RSP protein (VHH-RSP #3) and *Salmonella* cells harboring the R27 plasmid. **(B)** Transmission electron microscopy imaging mixtures of *E. coli* DH10BT1R cells expressing nanobodies against the RSP protein on its surface and cells of the *S*. Typhimurium SL1344 strain, harboring or not the R27 plasmid. The studies were performed by labeling the nanobodies producing bacteria (*E. coli* DH10BT1R) with a mouse antibody anti c-myc tag and goat anti-mouse IgG conjugated to 12 nm gold particles. Blue bars represent 1 µm while black bars represent 2 µm.

915

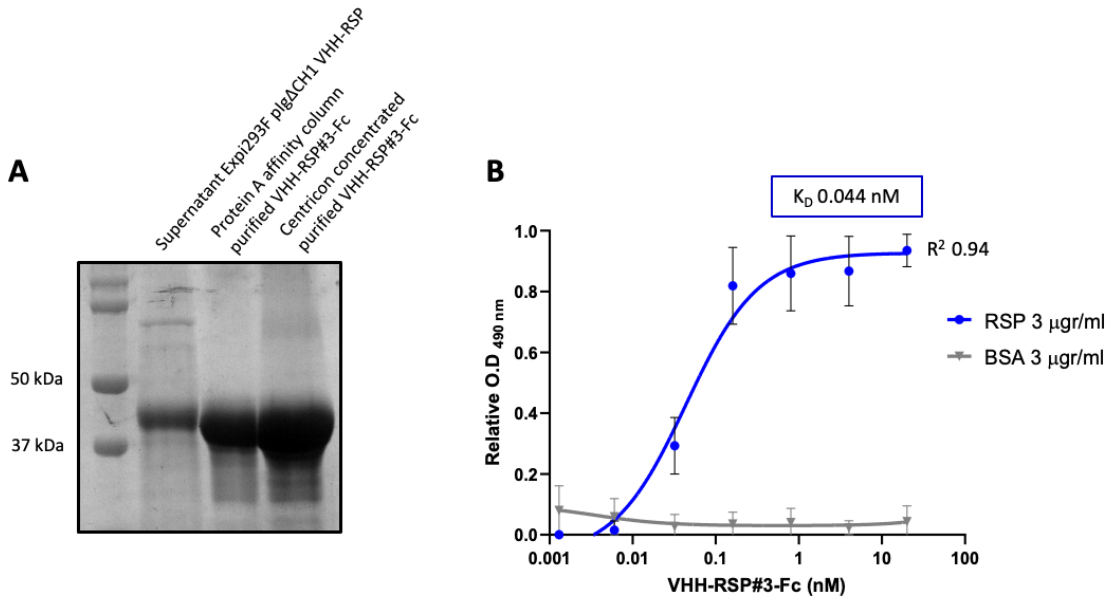

916

917 **Figure 8. Characterization of the purified VHH-RSP#3 as a specific binder to the RSP protein.**

918 **(A)** Purification of Nb3-Fc by affinity column**.** Coomassie staining of the SDS-PAGE (10%) showing

919 the purified Nb-RSP #3-Fc from transfected mammalian cell culture supernatants. Molecular

920 weight markers are indicated on the left. **(B)** ELISA showing the binding capacity of the purified

921 VHH-RSP#3-Fc to the RSP or BSA protein. The plot represents the OD values at 490 nm obtained

922 with the indicated concentrations of the purified Nb3-Fc after 1 hour of interaction with the

923 corresponding antigen.

924

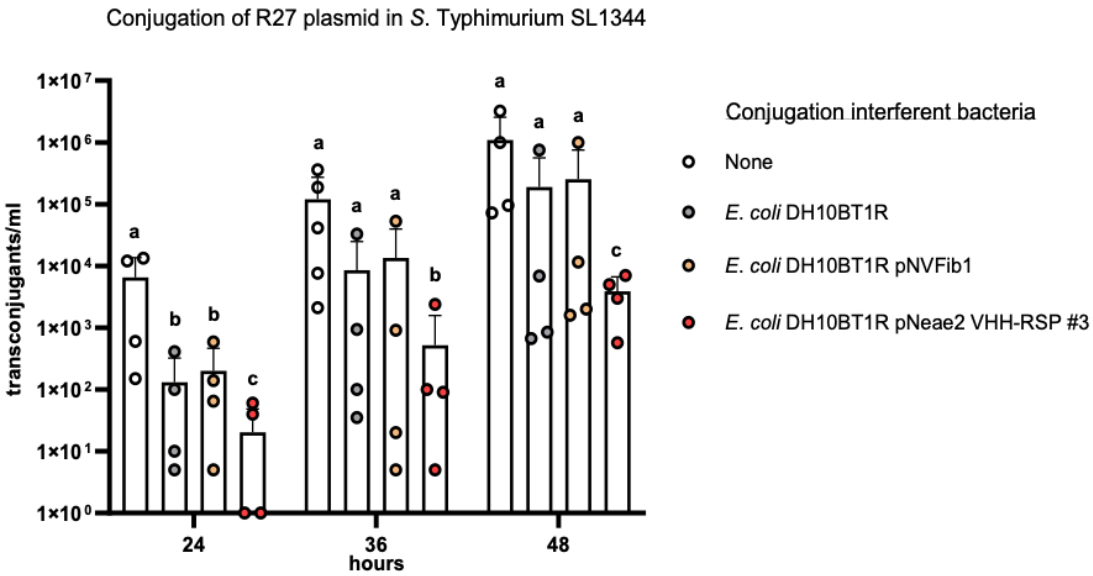

925

926 **Figure 9. Interference of *E. coli* DH10BT1R cells expressing nanobodies on its surface with the**
927 **conjugative transfer of the R27 plasmid in *Salmonella.*** R27 plasmid was conjugated from a
928 donor strain (SL1344) to a recipient strain (SL1344 *ibpA::lacZ-Km*^{r}) with the absence (labelled as
929 "none") or presence of the interferent strains *E. coli* DH10BT1R, plasmid-free clone; *E. coli*
930 DH10BT1R (pNVFib1), clone expressing a fibrinogen-specific VHH; *E. coli* DH10BT1R (pNeae2
931 VHH-RSP #3), clone expressing RSP-specific VHH. Means without a common letter differ, $P<0.05$.